University of Windsor Scholarship at UWindsor

Electronic Theses and Dissertations

Theses, Dissertations, and Major Papers

1989

Boiling initiation and hysteresis test facility.

Dinkar. Shivprasad University of Windsor

Follow this and additional works at: https://scholar.uwindsor.ca/etd

Recommended Citation

Shivprasad, Dinkar., "Boiling initiation and hysteresis test facility." (1989). *Electronic Theses and Dissertations*. 1321.

https://scholar.uwindsor.ca/etd/1321

This online database contains the full-text of PhD dissertations and Masters' theses of University of Windsor students from 1954 forward. These documents are made available for personal study and research purposes only, in accordance with the Canadian Copyright Act and the Creative Commons license—CC BY-NC-ND (Attribution, Non-Commercial, No Derivative Works). Under this license, works must always be attributed to the copyright holder (original author), cannot be used for any commercial purposes, and may not be altered. Any other use would require the permission of the copyright holder. Students may inquire about withdrawing their dissertation and/or thesis from this database. For additional inquiries, please contact the repository administrator via email (scholarship@uwindsor.ca) or by telephone at 519-253-3000ext. 3208.

|+] ∶ ¦

National Library of Canada

Bibliothèque nationale du Canada

Service des thèses canadiennes

Canadian Theses Service

Ottawa, Canada K1A 0N4

NOTICE

The quality of this microform is heavily dependent upon the quality of the original thesis submitted for microfilming. Every effort has been made to ensure the highest quality of reproduction possible.

If pages are missing, contact the university which granted the degree.

Some pages may have indistinct print especially if the original pages were typed with a poor typewriter ribbon or if the university sent us an inferior photocopy.

Reproduction in full or in part of this microform is governed by the Canadian Copyright Act, R.S.C. 1970, c. C-30, and subsequent amendments. AVIS

La qualité de cette microforme dépend grandement de la qualité de la thèse soumise au microfilmage. Nous avons tout fait pour assurer une qualité supérieure de reproduction.

S'il manque des pages, veuillez communiquer avec l'université qui a conféré le grade.

La qualité d'impression de certaines pages peut laisser à désirer, surtout si les pages originales ont été dactylographiées à l'aide d'un ruban usé ou si l'université nous a fait parvenir une photocopie de qualité inférieure.

La reproduction, même partielle, de cette microforme est soumise à la Loi canadienne sur le droit d'auteur, SRC 1970, c. C-30, et ses amendements subséquents.

Canadä



BOILING INITIATION AND HYSTERESIS -TEST FACILITY

.

BY

DINKAR SHIVPRASAD

C

A thesis

submitted to the \cdot

Faculty of Graduate Studies and Research through the Department of Mechanical Engineering in partial fulfillment of the requirements for the Degree of

Master of Applied Science at the

University of Windsor

Windsor, Ontario, CANADA

(C) D.Shivprasad, 1989

*

National Library

Canadian Theses Service

du Canada Service des thèses canadiennes

Bibliothèque nationale

Ottawa, Canada K1A 0N4

The author has granted an irrevocable nonexclusive licence allowing the National Library of Canada to reproduce, loan, distribute or sell copies of his/her thesis by any means and in any form or format, making this thesis available to interested persons.

The author retains ownership of the copyright in his/her thesis. Neither the thesis nor substantial extracts from it may be printed or otherwise reproduced without his/her permission.

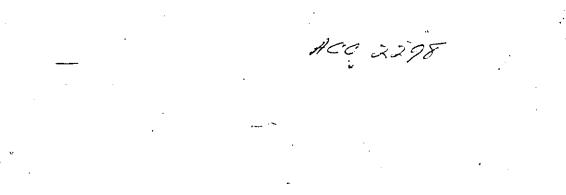
anadä

L'auteur a accordé une licence irrévocable et non exclusive permettant à la Bibliothèque nationale du Canada de reproduire, prêter, distribuer ou vendre des copies de sa thèse de quelque manière et sous quelque forme que ce soit pour mettre des exemplaires de cette thèse à la disposition des personnes intéressées.

£.

L'auteur conserve la propriété du droit d'auteur qui protège sa thèse. Ni la thèse ni des extraits substantiels de celle-ci ne doivent être imprimés ou autrement reproduits sans son autorisation.

ISBN 0-315-50534-6



1.

•



•

. . .

شر

Š.

ï

€. .

ABSTRACT

A forced convection heat transfer loop was designed to study the wall superheat necessary to initiate nucleate boiling, the wall superheat and heat flux at which nucleate boiling is quenched, and the hysteresis associated in a plot of heat flux versus local wall superheat during cycles of increasing followed by decreasing heat flux, using R-11 and R-113 as working fluids.

The test section flow is upward through a vertically oriented, concentric annulus, formed by a 22.2 mm outside diameter copper pipe, within a 25.4 mm inside diameter glass tube, 0.4 m long. The copper pipe is heated internally by a 76 mm long instrumented cartridge heater, which could be positioned anywhere along the length of the annulus test section.

The following system parameters can be varied within the ranges hown below:

1) System pressure (2 to 7.9 bars),

2) Inlet temperature (20 degrees C to the lesser of the saturation temperature or 100 degrees C),

3) Reynolds number in the test section (2900 to 25000 for R-11 and 2500 to 22000 for R-113),

4) Heat flux at the test surface (0 to 60 kW/m2).

A computer assisted data acquisition program was written to enable fast collection of information and in situ data reduction.

Preliminary tests were conducted with R-11 at 1.5 and 1.9 bar system pressures, 3 and 9 degrees C subcooling respectively and

iν

a Reynolds number of 3250.

It was observed from these preliminary runs that :

1) Boiling initiation required a finite, significant local wall superheat and the initiation was vigorous, all around the test surface. At higher flow rates and system pressures, the initiation becomes less vigorous.

2) Upon initiation, the wall superheat drops abruptly due to the higher heat transfer coefficient associated with boiling. For these tests, the wall superheat dropped to half of their previous value.

3) Increasing the wall heat flux with one or more sites already active results in a much different heat flux versus wall superheat relationship than for either cold startup or for cooling.

4) The disappearance of boiling at a site does not mean the site is quenched. Under some conditions, it will reactivate without the very large wall superheats required to initiate boiling from a quenched site.

ACKNOWLEDGEMENTS

The author wishes to express his profound appreciation to Dr. T. W. McDonald for his supervision, encouragement, patience and assistance throughout the course of this study. His ever Willingness to discuss the research project is greatly appreciated.

Special thanks to Dr. N. W. Wilson for writing the "FLUKES.BJO" machine language software and Dr. W. T. Kierkus for his invaluable insight and expertise during the course of this study.

The author wishes to extend his gratitude to M/s W. Beck, R. Tattersall and D. Liebsch for their professional and technical help in building the experimental setup.

Thanks are due to Dr. K. Sridhar for his friendy discussion and advice. Thanks are also due to all engineering graduate students for their informal discussion and friendship.

Acknowledgement is made to Natural Sciences and Engineering Research Council of Canada for providing financial assistance through Grant 877.

My final and most dearest expression of gratitude is to my Guru Sri Raghavendra Swami, my wife, parents, brother and sisters. Their inspirational encouragement and everlasting love and support made this endeavour possible.

Dedicated with love to

my Guru Jagadguru Sri Raghavendra,

my wife, son and my parents.

· · ·

· C

vii

· ·

TABLE OF CONTENTS

2

*		· .	
Abstract	-		(iv)
Acknowledgements) -		(vi)
Dedications	,		(vii)
List Of Figures			(xi)
Nomenclature			(xiii) ·
1. Introduction		~	1
2. Literature Review			6
2.1 Preamble	•		6
2.1.1 Flow regime up t	o incipient boiling f	or a	
a subcooled liquid	l in an uniformly heat	ed channe?	16
2.2 Review of previous	work	•	8
2.2.1 Surface			. 8
2.2.2 Role of surface t	ension and wettability	y '.	10
2.2.3 Influence of pres	sure temperature hist	ory	j 12
2.2.4 Mathematical mode	els in boiling nucleat	ion	13
2.2.5 Hysteresis effect	s.		16
3. Equipment Désign, Comm	issioning and Instrum	entation	20 `
3.1 Design objectives			20
3.2 General description	of the loop		21
3.3 Selection of working	; fluid		24
3.4 Component design			24
3.4.1 Test section			24
3.4.1.1 Test section h	eating conditions		25
3.4.1.2 Type of electr	ical heating		25
3.4.1.3 Type of electr	ical heater		25

viii

)		
3.4.1.4 Size of glass pipe	26	
• 3.4.1.5 Size of test pipe	26	
3.4.1.6 Size of main heater	27	
3.4.1.7 Copper sleeve	29	
3.4.1.8 Thermocouples for wall temperature measurement	: 31	5
3.4.1.9 Heater, thermocouple, sleeve assembly	33	
3.4.1.10 Heater positioning rod	33	
3.4.1.11 Test section sealing assembly	34	<i>ب</i>
3.4.1.12 Locking device for positioning rod	37	
3.4.2 Cooler	39	
3.4.3 Preheater	41	· v
3.4.4 System pressurizer	43	
3.4.5 Flowmeter	44	
3.4.6 Loop piping and fittings	47	·
3.4.7 Circulating pump	48	2
3.5 Instrumentation	50	
3.5.1 Temperature measurement	50	
3.5.2 Pressure measurement	52	
3.5.3 Data acquisition system	53	
3.6 Commissioning	56	
3.6.1 Leakage test	56	
3.6.2 Charging procedure	58	
3.6.3 Results of commissioning	60	
4. Results, Discussion and Conclusions	61	
4.1 Experimental procedure	61	
4.2 Results and discussion	63	
4.3 Conclusions and recommended future work	,72	
·		

· · ·	y
References	75
Appendices	N
A Dormancy mathematical models	78
B Heat loss through sleeve ends and push rod	84
C Test section end flange design	6 88
D Cooler sizing	91
E Flowmeter calibration curve	95
F Loop pressure drop calculations	97
G Pump, head-flow characteristic	102
H Data acquisition program	·
H.1 Flow chart	105
H.2 Nomenclature	106
H.3 Program listing	110
H.4 Sample output	115
I List of equipment and instrumentation	116
Vita Auctoris	119
`	

.

. مع

3-

×.

LIST OF FIGURES

¢

c

2,

1.1 Typical boiling curve	2
2.1 Flow regimes in an uniformly heated channel	7
2.2 Wedge type cavity	11
3.1 Schematic of experimental test facility	22
3.2 Overall view of the experimental setup	23
3.3 Machined sleeve	30
3.4 Test section	35
3.5 Test section assembly	36
3.6 Locking device for positioning rod	38
3.7 Cooler	40
3.8 Preheater	42
3.9 System pressurizer	45
3.10 Thermocouple plugs .	51
3.11 Data acquisition system for the experimental setup	55
3.12 Schematic of leakage test unit	57
3.13 Schematic of loop charging facility/	59
4.1 Photograph of the flow in the test section after	
bubble initiation	64
4.2 Photograph of the flow in the test section showing	
vigorous spontaneous boiling	65
4.3 Photograph of the flow in the test section before	
dormancy	66 [`]
4.4 Photograph of the flow in test section showing	
smoother transition to vigorous boiling \sim	67

ç

xi

- 4.5 Heat flux versus wall superheat for a pressure of 1.5 bars, 3 degrees C subcooling and 390 kg/s m2 mass flux
- 4.6 Heat flux versus wall superheat for a pressure of 1.9 bars, 11 degrees C subcooling and 390 kg/s m2 mass flux
- 4.7 Number of nucleation sites versus wall superheat for pressure of 1.5 bars, mass flux of 390 kg/s m2 and inlet subcooling of 3 degrees C
- A.1 Schematic of Hsu, Bergles and Rohsenow's model for boiling dormancy

_ xii

82

68

69

70

7\

	-		
		NOMENCLATURE	۰.
	A \	Parameter defined in equations A9, A10	
	A x	Cross sectional area (m ²)	
	в .	Flange inner diameter (m)	1
	C p	Specific heat (kJ/kg C)	
	D	Diameter (m)	
	f	Darcy's friction coefficient	
	f	Tensile strength (N/m ²)	
	g	Acceleration due to gravity (m/s^2)	
	G	Mass flux (kg/s m ²)	
	h 😞	Heat transfer coefficient (W/m ² C)	
	h fg	Latent heat of vaporization (kJ/kmol)	
	ĸ	Thermal conductivity (W/m C)	
	1	Equivalent length (m)	
	L	Cooler tube length (m)	
	'n	Mass flow rate (kg/s)	
,	p	Power (W)	
•	Р	Pressure (Bars)	
	Pr	Prandtl number	
	q	Heat flux (W/m^2)	
	Q .	Volumetric flow rate (m ³ /s)	
	r	Fouling coefficient	
	r,r _c	Cavity radius(m)	
	Re	Reynolds number	
	R	Universal gas constant (kJ/kmol K)	

٢

È

7

K

.

۱

<

xiii .

¢

Temperature(°C)

Velocity (m/s)

Overall heat transfer coefficient $(W/m^2 C)$

Distance from wall (m)

Parameter in Appendix-G

GREEK SYMBOLS:

Т

t

u

U

У

Y

β

δ

Δ

€

μ

Ω

θ

σ

υ

S.

Wedge angle (degrees)

Thermal boundary layer distance (m)

۲

Difference

Heat exchanger effectiveness

 λ Parameter in equation A5

Dynamic viscosity (kg/m s

Ratio of flange diameters

Contact angle between solid and bubble surface (degrees), measured through the liquid

ho Density (kg/m³)

Surface tension (N/m)

Specific volume (m³/kg)

xiv

2

Subscript:

ave Average value

f,1,1iq Liquid

fr Refrigerant

h, hyd Hydraulic

	. :
incp	Incipient
00	Beyond the boundary layer
min	Minimum
	A: A A A A A A A A A A A A A A A A A A
S	Saturation
sub	Subcooling
1,ss	Shell side
2,ts	Tube side
g,v	Vapour
w	Wall, Water
1	Inlet
2	Outlet

ć

XV

- ^{1,}

. **1**

`

x

٩

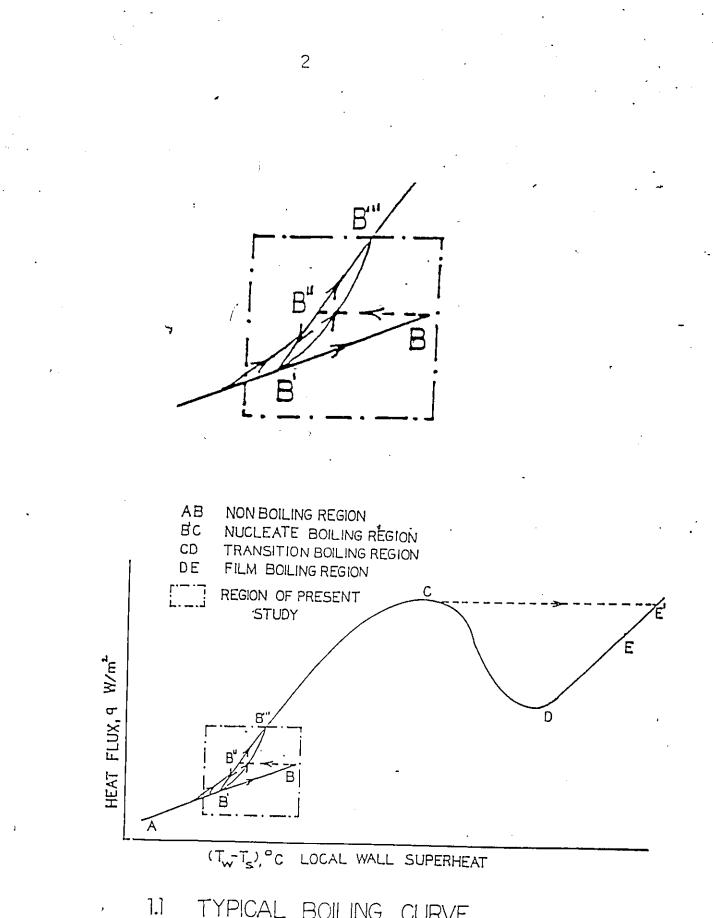
.

1. INTRODUCTION

The process of evaporation associated with vapour bubbles in a liquid is called Boiling.

Boiling heat transfer has been extensively studied in recent years because of many engineering applications which require high heat transfer ratès under moderate temperature differences (viz., nuclear reactors, rocket motors). The heat generated, in such applications must be removed to preserve the structural stability of the equipment. One method of removing this would be by single-phase forced convection flow. This, however, would require a large quantity of coolant and a large pump and motor. The same objective can be realized with a much lower flow rate if boiling is allowed (heat transfer coefficients typically ten times the single phase value). Also, uniform surface temperatures have been achieved in high speed computer components by their cooling them with boiling fluids.

One aspect of subcooled flow boiling which is not fully understood is the transition between convective heat transfer and nucleate boiling. When subcooled liquid is heated by an electrically heated wire or a flat plate, data for heat flux q versus local wall superheat (T_{w} - T_{m}), usually appear as shown in Figure 1.1. As the heat flux is increased, the initial forced convection regime A to B, changes to nucleate boiling regime. The appearance of the first bubble at B requires a significant finite local wall



TYPICAL BOILING CURVE

3

necessary to initiate nucleate boiling is known as the Incipient Nucleate Boiling Wall Superheat. However, once boiling has been initiated, there is a significant and abrupt fall in the local wall superheat, (Figure 1.1, from B to B). (Most textbooks present a simplified account of the boiling curve, showing a smooth transition from A to B , ignoring the B to B transition). As (T_- T_), or the heat flux, is increased, more nucleation sites become active producers of bubbles. A peak nucleate boiling heat flux is reached at point C. At this point, if any further increase in heat flux occurs, the bubbles stream forth from so many sites that the liquid is unable to flow to the heated surface and film boiling takes over at point E, which is at a much higher wall superheat. Operation in C-D-E region is achieved only if wall superheat is the independent variable.

If we decrease the heat flux from point C, it is observed that the curve C to B to B to A is not retraced. Instead, the path C to B to B to A is followed. At B, the last nucleation site disappears. The superheat at which a nucleation site disappears is known Nucleate Boiling Dormancy Wall Superheat. as the site Nucleation sites which are dormant will reactivateup on a much smaller increase in wall superheat than that required to initiate a quenched site. When such sites reactivate, a smooth transition occurs from state B, to state B , as the dormant sites initially reactivate then subsequently, the vapour streams from these sites reactivate others downstream. At B much of the

surface is still not boiling. If the liquid is further subcooled below B^{1} , all the nucleation sites may become quenched, depending upon the amount of subcooling. When this happens, a wall superheat, the same as that for "cold" startup will be required to reactivate the site. In this case, path $B^{'}$ to B to $B^{''}$ will be retraced. The superheat at which a nucleation site is quenched is known as the site <u>Nucleate Boiling Quench Wall Superheat</u>. Between these two extremes of all nucleation sites being dormant or, all sites quenched, depending on the amount of subcooling after dormancy, we have cases of some sites being dormant and others quenched. Depending on their relative numbers, we have different boiling transition curves from non boiling to nucleate boiling region.

Thus we observe that the wall superheat necessary for boiling incipience is quite different from the superheat at which the site disappears, and the loop B^{\dagger} to B to B^{\dagger} to B to B^{\dagger} , is an example of a Boiling Curve Hysteresis.

McDonald et al. [14], in order to simulate the experimental results of their previous work [13], formulated a <u>Quench/ Dormancy Model</u>, in which they assumed that when the local wall superheat falls below some fraction, of the superheat at which a site becomes dormant, then the nucleation site is quenched, otherwise the nucleation site is dormant. A subsequent increase in wall superheat will cause a reactivation of dormant sites, but the quenched sites will require a local wall superheat

ļ

approximately equal to that required to initially activate them.

The objective of the present study is to design, test and . commission a forced convection heat transfer loop which may be used to study individual nucleation sites for the following : 1) the incipient nucleate boiling wall superheat,

2) the nucleate boiling dormancy wall superheat, and nucleate boiling quench wall superheat,

3) the hysteresis associated with the above phenomena for cycles of increasing followed by decreasing heat flux,

4) the verification of the quench/ dormancy model,

so that a better understanding of these phenomena and their mechanisms is achieved. Once understood, one would be able to develop an engineering model which would allow these phenomena to be simulated on a computer.

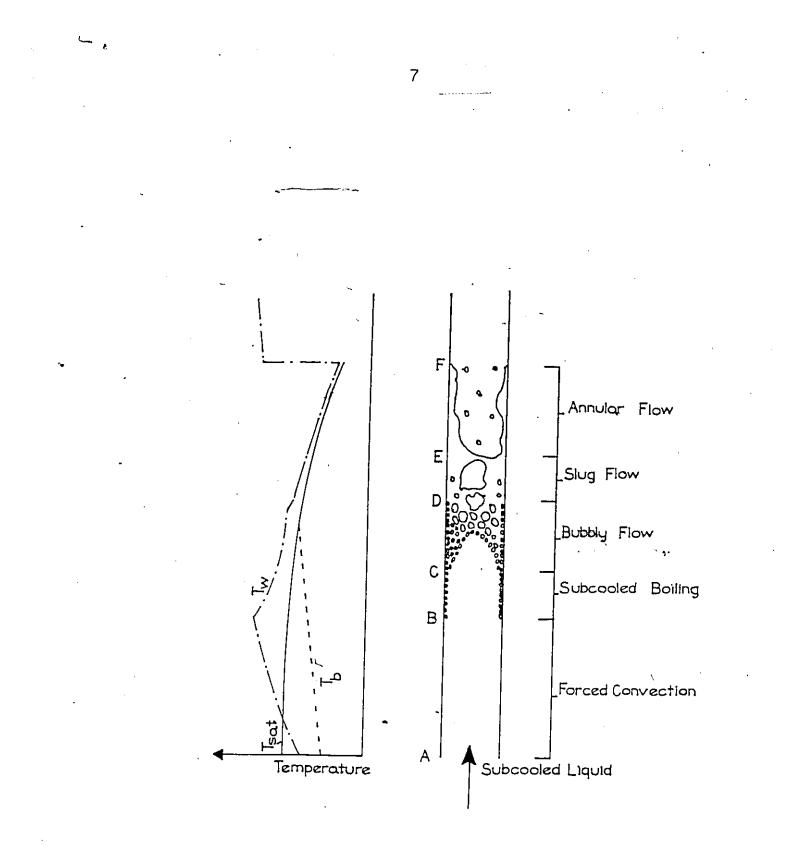
A review of literature in the areas of incipient boiling wall superheat, hysteresis in the transition region from forced convection heat transfer to nucleate boiling is presented first. In the following chapters, the heat transfer loop design and commissioning, the required instrumentation for the loop, the results obtained from preliminary runs, and conclusions from the present study and recommendations for further study, are discussed.

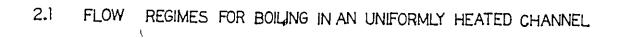
2. LITERATURE REVIEW

2.1 Preamble

2.1.1 Flow Regime Up To Incipient Boiling For A Subcooled Liquid In An Uniformly Heated Channel

In order to understand the behaviour of individual nucleation sites in flow boiling, it is necessary to know the flow regimes that occur for a subcooled liquid in an uniformly heated channel. In Figure 2.1, subcooled liquid enters the bottom of a uniformly heated vertical tube. From A to B, the heat transfer is entirely by single phase forced convection, since the wall temperature, though higher than saturation temperature, is still below the value necessary for bubble nucleation. At B, the wall temperature reaches a superheat high enough to initiate nucleation. There is a sharp drop in local wall temperature at each site. At B, the bulk liquid is still highly subcooled, so vapour bubbles are confined to the wall region, often sliding along the wall as they grow. Bubbles that detach recondense, as they enter the main stream. At C, the bulk temperature, although below T , has increased sufficiently for bubbles to exist in the main flow. At this point there is a sharp increase in the void fraction. Between C and D, T reaches T, and bubbles no longer condense as they leave the wall. Bubble coalescence leads to slug flow (D toE) followed by annular flow (E to F) in which a thin liquid film covers the tube wall, while vapour, liquid droplets flow up the centre at high velocity. The regime (A to C), is the region that exists in the





test section to be discussed in the present thesis.

2.2 Review Of Previous Work

A large number of research workers have contributed to our understanding of various phenomena in the "knee" region of the boiling curve. The phenomena of nucleate boiling wall superheats have been studied in both pool boiling [4,7,9], and flow boiling [1,2,10,15,16]. Also, studies have been carried out on hysteresis in pool boiling [7,12], flow boiling [11,17] and in thermosyphon loops [13,14].

The variables affecting incipient boiling wall superheat may be classified in the following manner:

2.2.1 Surface

£

2.2.1.1 Geometry

Incipient boiling is insensitive to system geometry, provided the surface dimensions are larger than typical bubble sizes (1 mm for water at atmospheric pressure) and the bubbles are able to escape from the heated surface [6].

2.2.1.2 Effect Of Surface Conditions

Surface finish has a pronounced effect on incipient boiling by altering the number of nucleation sites, but at present there is insufficient material in the literature to put it in a quantitative basis. Studies have been performed involving boiling enhancement surfaces[30] (surfaces which reduce the incipient boiling wall superheat).

Corty and Foust[7] have reported the effects of surface roughness on the boiling curve for several fluid-surface combinations. In these experiments, saturated, pool boiling of diethyl ether, n-pentane, and R-113 were investigated from an upward facing, horizontal plate which had first been plated with either copper or nickel, then roughened by rubbing with various grades of emery paper. Their results indicated major а influence of microroughness on the wall superheat necessary to initiate # nucleate boiling at any given heat flux. For an n-pentane/ nickel interface, with a 0.056 μm root mean square surface roughness, nucleate boiling started at a local wall superheat of 19.67 degrees C, while a surface with 0.58 μ m root mean square roughness required a local wall superheat of 28.89 degrees C. They said. this was probably because the rougher surfaces contain larger cavities, and hence are easily filled with liquid and are therefore unable to trap vapour.

Howell and Siegel[4] studied the effect of the size and geometry of nucleation sites for a stainless steel AISI 410, water combination, in pool boiling. Two types of artificial sites were studied. The first was drilled by electron beam and the site diameter was 63.5 μ m and the second type was 76.2 μ m diameter produced by a mechanical drill. In most of the test strips, two sites of the same nominal diameter were drilled about 25.4 mm apart. Three strips were tested with different site diameters, to

7

observe the effect of site diameter under identical test conditions. Low heat fluxes were used near incipience so that it was possible to grow isolated bubbles. They concluded that larger cavities are filled with liquid before vapour replacement can take place, making the cavities inactive.

2.2.2 Role Of Surface Tension And Wettability

Bankoff [8] gives criteria to characterize conical or wedge type cavities (with β , conical or wedge angle as the case may be, refer to Figure 2.2) as to their abilities to trap vapour. The ability to trap vapour depends to a large extent on the contact angle θ , between the bubble interface and the solid wall measured through the liquid, and the wedge or cone angle as the case may be. Angle θ , is determined by the force balance between the surface tension forces of the vapour/ liquid/ solid interface.

١

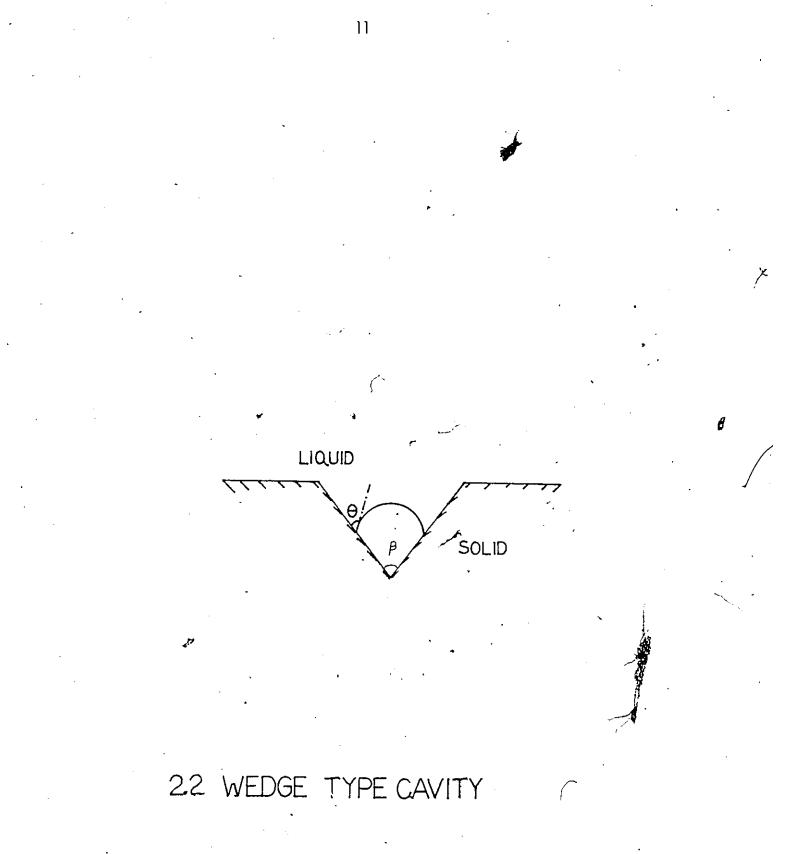
The above mentioned cavities can be classified in one of four categories, depending on whether or not they obey the following inequalities:

 $\theta > \beta$

and

 $\beta > \theta' - \pi$

 Those which obey the first inequality but not the second (Poorly wetted, shallow)-vapour entrapment not possible.
 Those which obey the second inequality but not the first (Well wetted, steep slope)-possible to switch from liquid



.

to gas filled cavity.

5

3) Those which obey both (Poorly wetted, steep slope)complete displacement of liquid or gas, once filled is not possible.

4) Those which obey neither (Well wetted, shallow)entrapment of vapour not possible.

2.2.3 Influence Of Pressure Temperature History

Sabersky and Gates[9] performed experiments with 2.54 mm diameter platinum and nichrome wires which were immersed in a vessel filled with water. The assembly was subjected to a pressure of 1035 bars for periods in excess of 15 minutes. The pressure was then reduced to atmospheric and the wire heated electrically. They found that the superheat for boiling incipience was 35 degrees C for a distilled water/nichrome wire combination and about 63 degrees C for a tap water/platinum wire combination. Further, they ran tests with unpressurized water and concluded that the pressurization treatment eliminated the more effective sites, through gas dissolution or vapour condensation. Once boiling has begun, and the surface has again been exposed to vapour masses, the larger cavities will reactivate and further boiling will occur at surface temperatures encountered before pressurization.

Cher [10] performed experiments to determine the effect of subcooling and prepressurization on incipient nucleate boiling superheat. The measurements were made for potassium in forced convection flow. He found that increasing subcooling or prepressurization causes higher subsequent superheats at boiling inception. In his experiments, the subcooling was between 0-220 degrees C, prepressurization between 0-275 bars and the measured superheats ranged between 9.5-65 degrees C.

2.2.4 Mathematical Models In Boiling Nucleation

N

Each of the above mentioned studies have contributed to the understanding of the parameters which influence bubble nucleation but a quantitative relationship between the basic surface parameters and the heat transfer was not found. In the work of Hsu[2], Bergles and Rohsenow[15], Davis and Anderson[16], and Sato and Matsumura[1], an attempt was made to establish a relationship between cavity radius, wall temperature, and heat transfer rate to determine the range of cavity sizes that qualify as active sites and predict the nucleate boiling dormancy. Readers may please note that, all the above mentioned authors [1,2,15,16] have erroneously referred to nucleate boiling dormancy as incipient nucleate boiling in their literature. All of them assume that a vapour bubble is <u>already</u> present, and give the criteria for bubble growth. Refer to Appendix-A for further details on the analytical model developed by Hsu, and Bergles and Rohsenow.

Hsu[2] postulated that the bubble nucleus grows only when the surrounding liquid is sufficiently superheated, so that there is a net heat flux transferred into the bubble to provide the heat of viporization. He calculated the local liquid temperature by one

dimensional transient conduction in a thermal layer. He proposed

$$q = \frac{k \left[\zeta + \xi + (2\zeta + \xi) \xi \right]}{\delta}$$
where, $\zeta = (T_{g} - T_{b})$ and
$$\frac{\xi - 4 \sigma T_{g} (1 + \cos \theta)}{h_{e_{g}} \rho_{y} \delta}$$

To determine the heat flux by his method, it is necessary to know the contact angle θ and thermal layer thickness δ , both of which are in general difficult to determine.

Bergles and Rohsenow [15] assumed a steady temperature gradient and adopted the procedure developed by Hsu to develop a criterion for nucleate boiling dormancy heat flux for surfaces with a wide range of cavity sizes.

From their experiments for incipient nucleate boiling they arrived at the following correlation for water over a pressure range of 15-2000 Psia.

$$q = \frac{15.6 P^{1.156} (T_{w} - T_{s})^{2.3}}{P^{0.0234}}$$

where q, is in Btu/hr ft2; P is in Psia and T is in degrees F. They employed a graphical method from which they predicted incipient nucleate boiling dormancy superheat and the cavity size that is active, before nucleate boiling dormancy begins. Kenning [6] suggests that using the procedure of Bergles and Rohsenow, we can predict incipient nucleate boiling superheat, if we assume $1 \ \mu m$ as optimum cavity size.

Sato and Matsumura[1] proposed an analytical formulation similar to Hsu's for prediction of nucleate boiling dormancy. They assumed:

1) That the temperature profile in the thermal layer is steady and linear,

2) The vapour bubble is hemispherical and its radius is half of the superheated layer thickness.

They obtained the following equation for nucleate boiling dormancy heat flux,

$$q = \frac{k h_{fg} (T - T_{g})^{2}}{8 \sigma T_{g} (v_{v} - v_{l})}$$

An analysis of nucleate boiling dormancy was developed by Davis and Anderson[16] as a modification and extension of previous analyses. They assumed a truncated spherical bubble, and derived the following equation for the prediction of subcooled boiling of water in forced convection

$$q = \frac{k h_{fg} \rho_v (T_v - T_g)^2}{8 \sigma T_g (1 + \cos \theta)}$$

where θ , is the contact angle between bubble and the surface.

They used the data from Sato and Matsumura[1], for comparison with their analysis and ,it may be concluded that their analysis predicts the local wall superheat required for nucleate boiling dormancy.

It may be concluded that, the thermodynamic requirements considered by Bergles and Rohsenow, Hsu, Davis and Anderson, Sato and Matsumura are capable of predicting nucleate boiling dormancy superheat and there are no models available in the literature for predicting incipient nucleate boiling wall superheat, and nucleate boiling quench superheat.

2.2.5 Hysteresis Effects

Corty and Foust[7] observed the difference in behaviour of nucleation centers under certain conditions, depending upon whether the heat flux was increasing or decreasing. While increasing heat flux, the wall superheat necessary for boiling inception was higher than that required to maintain boiling during decreasing heat flux.

Abdelmessih[11] et al. experimentally observed hysteresis in an electrically heated, horizontal, stainless steel AISI 304 tube test section using R-11 in forced flow. A wall superheat of 13.8 degrees C to 16.7 degrees C above the local saturation temperature was found necessary to initiate boiling in their test facility. Once local boiling was initiated, the wall superheat dropped substantially. This nucleate boiling could be sustained even when

the wall heat flux was reduced to the point where the tube wall temperature fell within a few degrees of the local saturation temperature.

Joudi and James[12] carried out investigations on a flat horizontal stainless steel surface of known roughness. The system pressures for the tests were 0.25 bars, 0.5 bars, and 1.0 bar. At 1 bar system pressure, they observed that wall superheats of approximately 16 degrees C for R-113 and 19 degrees for methanol were required to initiate boiling.

Hino and Ueda [17] carried out the study on upward subcooled flow boiling in an annulus with a uniformly heated inner tube. The test fluid was R-113. The wall temperatures were measured and photographic observations carried out. They made the following observations:

1) The wall superheat at the position of incipient boiling is relatively high, and a sharp drop in wall temperature takes place after boiling initiation.

2) The wall superheats at the incipient boiling condition are virtually independent of the mass flux and the inlet subcooling.
 3) Hysteresis occurs for complete cycle of increasing followed by decreasing heat flux.

Stauder and McDonald [13] studied the onset of nucleate boiling of R-11 for a thermosiphon heat exchanger. The experiments were

carried out on a 4 loop, 2 row of tubes per loop, prototype commercial air-to-air thermosiphon heat exchanger. They found that, for an R-ll/ copper interface, a hot duct to cold duct temperature difference of 16 degrees C to 17 degrees C was required to initiate boiling for operating pressures between 1.2 bars and 1.6 bars. Once initiated, however, boiling was sustained until the air-to-air temperature difference decreased to 4 degrees C. This hysteresis behaviour was exhibited when operating with temperature differences below 50 degrees C. Upon reheating, in this region, a portion of the nucleate sites previously made inactive reactivated easily whereas others were completely quenched.

McDonald[14] et al. simulated the experimental results of their previous work[13], and using a quench/ dormancy model, found good agreement with the experimental results in the hysteresis region. In that model, they assumed that when the local wall superheat falls below some fraction, say P, of the minimum wall superheat necessary to maintain nucleate boiling, then the nucleation sites are quenched, otherwise the nucleation sites remain dormant. A subsequent increase in wall superheat will cause a reactivation of the dormant sites, but the quenched sites will require a local wall superheat approximately equal to that required to initially activate them.

In conclusion we might say that the subcooled flow boiling is a complicated nonequilibrium state involving the vapour bubbles and the subcooled liquid. Though each of the above mentioned studies

.18

have contributed to our understanding of the various phenomena in the "knee" region of the boiling curve, subcooled boiling phenomena have not yet been understood completely in detail. None of the previous investigators have developed models for :

1) Incipient nucleate boiling wall superheat,

2) Nucleate boiling quench wall superheat,

۲.

72

3) Conditions under which a nucleation site is dormant, and the conditions under which it is quenched. The present study was undertaken to throw additional light on the behaviour of individual nucleation sites and the heat transfer in subcooled flow boiling, so that models can be developed which will allow these phenomena to be simulated on a computer.

3. EQUIPMENT DESIGN, INSTRUMENTATION AND COMMISSIONING

3.1 Design Objectives

A heat transfer loop was designed and commissioned to study the, following phenomena:

1) Incipient boiling wall superheat,

2) Boiling dormancy and quench wall superheats,

3) The hysteresis associated with a plot of heat flux versus local wall superheat, for a complete cycle of increasing followed by a decreasing heat flux. The ultimate overall objective is to gain a better understanding of these phenomena so that a practical quench/ dormancy model may be established which may satisfactorily predict the hysteresis phenomena.

The loop was designed so that these phenomena could be studied as a function of the following parameters :

1) Heat flux at the test surface,

2) System pressure at the test section inlet,

3) Subcooling at the test section inlet ,

4) Reynolds number in the test section ,

5) For both a developed or a developing flow field at the test section.

In order to observe the boiling, it was decided that the flow be annular between an inner heated surface and an outer glass pipe.

For data evaluation and analysis, it was decided that the

following parameters be controlled:

1) System pressure ,

2) Volumetric flow rate ,

3) Heat flux ,

4) Location of heater,

and the following parameters be calculated or measured:

1) Inlet subcooling at the test section ,

2) Reynolds number in the test section ,

3) Incipient boiling wall superheat ,

4) Boiling quench wall superheat ,

5) Incipient boiling heat transfer coefficient,

6) Boiling quench heat transfer coefficient,

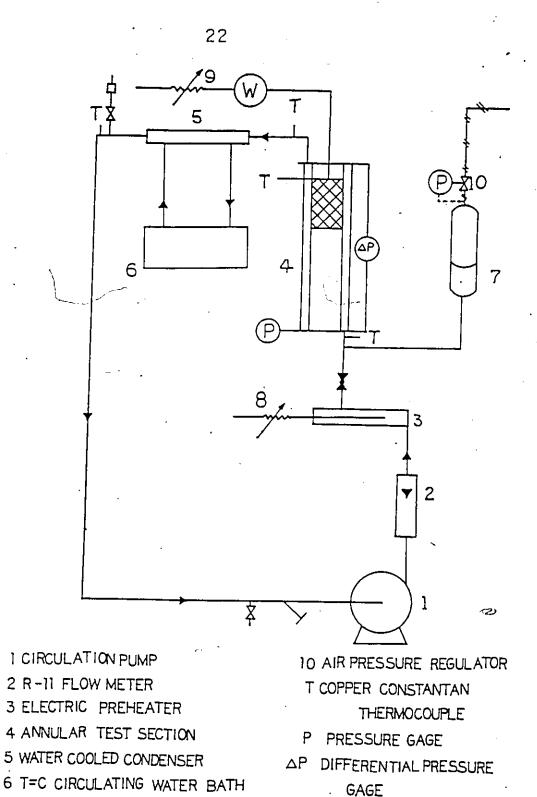
7) The location of both incipient boiling, and of boiling dormancy.

3.2 General Description Of The Loop

A schematic of the heat transfer loop is shown in Figure 3.1. The flow circuit is a closed circulation loop and is in one vertical plane. Figure 3.2 shows overall views of the test assembly.

The loop is designed to operate at a maximum working pressure of 7.9 bars (100 Psig) and a maximum working temperature of 120 degrees C. Refrigerant-11, with a latent heat of vaporization of 37.53 kJ/kg and a boiling point of 23.63 degrees C at 1 bar pressure was chosen as the working fluid.

The design details of each component is presented in the following



- 7 AIR MODULATED PRESSURIZER
- 8,9 VARIACS
- 3.1 SCHEMATIC OF EXPERIMENTAL TEST FACILITY

W WATTMETER

National Library of Canada

Canadian Theses Service

NOTICE

ر

THE QUALITY OF THIS MICROFICHE IS HEAVILY DEPENDENT UPON THE QUALITY OF THE THESIS SUBMITTED , FOR MICROFILMING.

UNFORTUNATELY THE COLOURED ILLUSTRATIONS OF THIS THESIS CAN ONLY YIELD DIFFERENT TONES OF GREY. Bibliothèque nationale du Canada

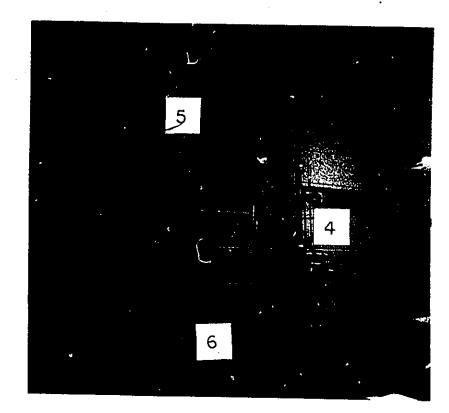
Service des thèses canadiennes

AVIS

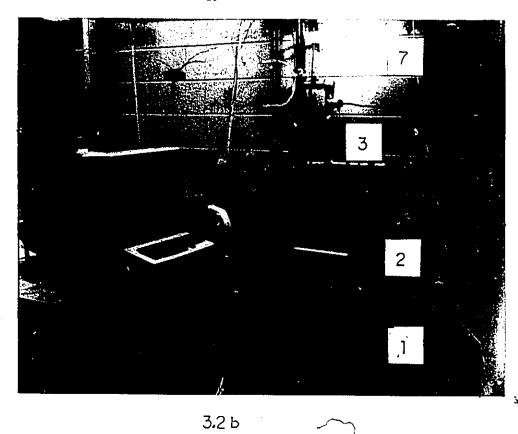
4

LA QUALITE DE CETTE MICROFICHE DEPEND GRANDEMENT DE LA QUALITE DE LA THESE SOUMISE AU MICROFILMAGE.

MALHEUREUSEMENT, LES DIFFERENTES ILLUSTRATIONS EN COULEURS DE CETTE THESE NE PEUVENT DONNER QUE DES TEINTES DE GRIS.



3.2 a.



3.2 OVERALL VIEW OF THE EXPERIMENTAL SETUP

·23

sections. Appendix-I lists the specifications of the equipment designed and used in the present study.

3.3 Selection Of Working Fluid

In order to observe the boiling phenomena it was decided that the test section be inside a glass pipe. With this in mind it was therefore necessary to operate the system close to room temperature to minimize heat losses so that no insulation is required in the test section. This in turn meant that a working fluid be chosen which has a low saturation pressure at room temperature, since low pressure operation was considered essential for reasons of safety. It is also desireable for the test fluid to have a low latent heat of vaporization so that the heater and condenser sizes may be small and easy to control.

a wide range of the two phase region, and they also have a low toxicity. They are relatively cheap and easily available. Hence it was decided that the loop will be designed for R-11 and R-113.

3.4 Component Design

3.4.1 Test Section

As already mentioned in Section 3.1, in order to observe the boiling phenomena, it was decided that the flow be annular between an inner heated pipe and an outer glass pipe.

The following additional factors were considered in designing the

`test section.

3.4.1.1 Test Section Heating Conditions

Electrical heating imposes constant a heat flux_ boundary condition. while fluid heating imposes constant temperature boundary conditions. If one type of boundary condition is imposed then the other parameter must be measured for data evaluation and analysis of results. It was found from [19] that the results from the two heating methods are not different from one another. Since it is physically easier to control and measure constant heat flux boundary conditions than constant temperature boundary conditions, igewas decided to use electrical heating.

3.4.1.2 Type Of Electrical Heating

Direct electrical heating requires a low voltage high current supply (hundreds to thousands of amperes), especially for thick walled low electrical resistance channels. At present, the heat transfer research laboratory at the University of Windsor does not have such facilities. The option of using a high resistance, thin wire was eliminated because, as mentioned in Section 2.2.1.1, the nucleate boiling results are sensitive to system geometry especially if the surface dimensions are smaller or comparable with the bubble dimensions. Hence, it was decided to use indirect electrical heating.

3.4.1.3 Type Of Electrical Heater

Since it was decided that we should be in a position to study boiling in both developing and developed velocity profile regions.

it became necessary that we could position the heater anywhere along the length of the test section. Based on the considerations so far, it was decided to use a cartridge heater. These heaters allow a good thermal contact between the heater and the test pipe.

3.4.1.4 Size Of Glass Pipe

From the manufacturer's catalogue it was found that as the nominal size of the glass pipe increases, its maximum working pressure decreases. Thus a bigger diameter pipe reduces the test condition range. However, it should be big so that it can house test sections of different diameters.

At 7.91 bars (100 Psig), the saturation temperature of R-11 is 98.17 degrees C. Since water is being used as the coolant in the cooler(to be discussed in section 3.4.2) 98.17 degrees C is the maximum temperature and 7.91 bars is the maximum pressure under which we can run experiments. Hence, 25.4 mm (1 in) internal diameter, QVF (Quick Visible Flow) glass pipe supplied by Peagasus Industrial Specialities, Agincourt, Ontario with a maximum working pressure of 7.91 bars and maximum working temperature of 300 degrees C was selected.

3.4.1.5 Size Of Test Pipe

١.

As mentioned in section 2.2.1.1, incipient boiling is insensitive to system geometry provided the surface dimensions are larger than <u>f</u> typical bubble sizes(1 mm diameter). So it was decided to use pipe

of large diameter.

F

The outside diameter of the test pipe should be such that the resulting hydraulic diameter, hence the Reynolds number, should be in the range of interest (3000 to 30000, as this is the typical Reynolds number range existing in most industrial evaporators and condensers).

- 92

With a hydraulic diameter of 3.2 mm and the flow rate the pump is capable of delivering (refer to section 3.4.10), it was possible to achieve approximately the desired Reynolds number range (2871 < Re < 28710 for R-11 and 2475 < Re < 24750 for R-113, at 20 degrees C).

The length of the annulus should be such that it allows for a smooth transition from plug flow to annular flow, and also allows the velocity profile to develop completely. From [21], the length for complete velocity profile development was found to be 20 hydraulic diameters.

Based on the above criteria, the test pipe was chosen from commercially available copper pipe, 22.225 mm (0.875 in) external diameter, 19 mm (0.75 in) and 0.762 m (30 in) long.Since the glass pipes are available in few selected lengths, a 0.4572 m (18 in) long pipe was selected. Please refer to Figure 3.5.

3.4:1.6 Size Of Main Heater

It should be capable of supplying a heat flux which will result in nucleate boiling -i.e., higher than 35kW/m2 [18]. It should supply less power to the working fluid, so that the bulk temperature of the fluid, evaluated over the volume, and the inlet subcooling, do not change appreciably as it passes through the test section. This is necessary because we use conditions at test section inlet as parameters, and do not want these parameters to change.

The length of the heater should be shorter than the length required to fully develop a temperature profile, so that the bulk temperature, evaluated over the cross section, is approximately the same as the one at inlet to the test section.

The thermal boundary layer thickness was determined for R-11, under minimum anticipated flow conditions, using the correlations from [19] for various heated surface lengths. It was found that this thickness is 1 mm at 63.5 mm (2.5 in) heated length. This therefore was decided as the upper limit for the cartridge heater length...

A boiling heat transfer coefficient of 1500 W/m2 C was assumed on the basis of results from [20], and a wall superheat of 18 degrees C, for boiling initiation on the basis of results from [11]. Thus a heat flux of 27000 W/m2 was found necessary at the boiling surface for boiling incipience.

For various cartridge heaters, the heat flux available at the test surface, and the bulk fluid temperature rise as it passes through the test section was determined.

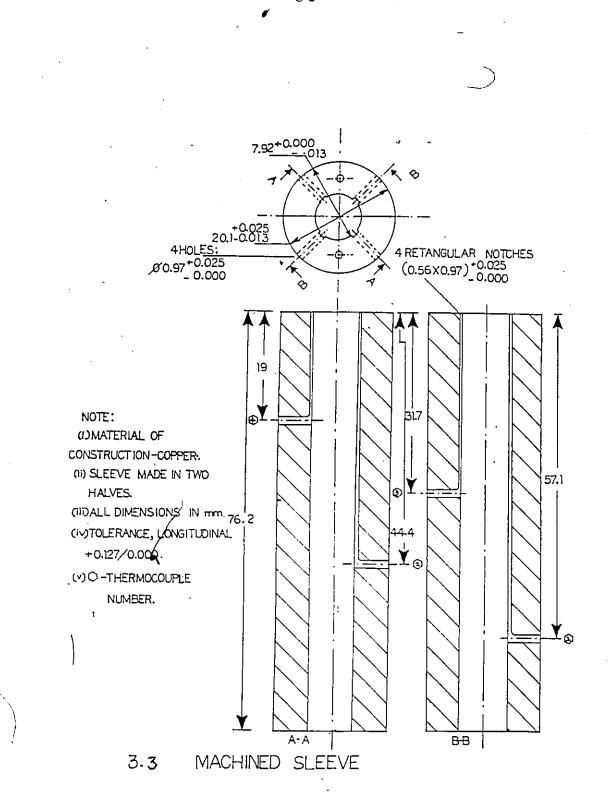
Finally, a H1-3, Fastheat, "Hi-Temp" cartridge heater with 7.874

mm (0.31 in) diameter, 76.2 mm (3 in) sheath length and 63.5 mm (2.5 in) heated length, capable of delivering 49972 W/m2 at the test surface 225 W rating at 120 V ,supplied by Acrolab Instruments, Windsor, Ontario was selected. At minimum flow, the flowmeter is capable of measuring (refer to section 3.4.5) and zero subcooling, the heat flux necessary for boiling initiation for R-11 was determined using Sato and Matsumura's [1] equation. At this heat flux, with this heater, the bulk temperature rise of the fluid was found to be 0.384 degrees C.

The power supply for the heater was through a Variac capable of delivering between 0-140 V. The power input to the heater was measured by a wattmeter capable of measuring 0-250 W with an accuracy of +/-1.25 %.

3.4.1.7 Copper Sleeve

In order to house the instrumentation for measuring the heated surface temperature, a sleeve was designed. The sleeve shown in Figure 3.3 was made of copper so that the temperature drop across the sleeve would be small, and hence avoid excessively high temperatures in the heater element. Four thermocouples, one each in a slot, running along the length, each separated by 90 degrees, were installed at equal lengths along the sleeve to measure the temperature of its outside surface. This meant that to measure the wall temperature at a nucleation site accurately, the thermocouple orientation would have to be changed by the experimentor accordingly. The arrangement of thermocouples running parallel to the test section also reduces thermocouple conduction errors.



These slots introduce discontinuity in the heat flux lines. To minimize this, thin wire thermocouples were selected. For the same reason it was decided to cut the slots at the inner surface of the sleeve, so that the heat flux lines are almost radial by the time they reach the sleeve outer surface and hence inner surface at the test section. Since thin slots are difficult to machine at the sleeve inner surface with accuracy if it is in one piece, it was decided to machine the sleeve in two equal halves and then cut the thermocouple slots.

One thermocouple was installed at the top of the sleeve, close to the sleeve inner surface. The temperature indicated by this thermocouple guides the experimentor if he can safely increase the heater power without damaging the heater element and also without damaging the soft solder which joins the heater/ sleeve assembly (to be discussed subsequently).

The external diameter of the sleeve was 20.066 mm (0.79 in) +0.000 mm/-0.1016 mm (0.004 in). This was the recommended tolerance [22] between mating parts for a locational clearance fit(a fit which allows good mating and easy positioning at the same time) for a 20.066 mm diameter shaft.

3.4.1.8 Thermocouples For Wall Temperature MeasurementThe desirable properties of a thermocouple sensor are :1) It must have a high Seeback coefficient,

2) It must have fast response to follow temperature changes accurately.

For a thermocouple, the response time is reduced only by reducing the wire diameter. However, as wire size is reduced to AWG (American Wire Gage) 36 and above, the junction becomes fragile and life shortened [23].

Type-T (Copper/Constantan-55% Copper and 45% Nickel) was selected because it has a moderately high Seeback coefficient of 38μ V/C at 0 degrees C, with limits of error +/-0.5 C or 0.4% (whichever is greater). For the range of operation the error was therefore +/-0.5 degrees C. Teflon thermocouple insulation was chosen because it retains its dielectric properties up to 260 degrees C, and also has excellent resistance to solvent, acid, base, abrasion, water and is flexible. Thermocouple TT-T-30(type T, teflon insulation, 30 AWG size) supplied by Omega Engineering Company, Stamford, Connecticut was therefore selected.

For an accurate outside wall temperature measurement, the thermocouple sensing tip was soldered at the sleeve outside wall. Also, the two halves of the sleeve were soldered rather than bolted, to avoid any nonuniformity in the heat flux at the test surface.

To reduce any temperature drop due to air gap (if any) between the heater outer surface and sleeve inner surface and also between the sleeve outer surface and test inner surface, a coat of

Omegatherm-201 thermally conducting paste. supplied by Omega Engineering Inc.,Stamford,Connecticut was applied.⁴ This paste had a thermal conductivity of 2.31 W/m C , and was capable of continous operation up to 205 degrees C. The temperature drop across the gap while the heater delivers 225 W, was estimated at 1.03 degrees C using one dimensional steady state thermal conduction equations.

3.4.1.9 Heater, Thermocouple, Sleeve Assembly

The assembly sequence for the heater, thermocouples, sleeve unit was as follows :

1) The thermocouple tips were soldered to the sleeve wall using silver solder (45 % silver, 15 % copper, 24% cadmium, 16% zinc) with a melting point of 604 degrees C,

2) A coat of thermally conducting paste was applied to the sleeve inner surface,

3) A thin coat of soft solder (62 % tin and 38 % lead) was applied on the mating faces of the sleeve halves,

4) The sleeves were joined and heated by a flame torch, melting the solder applied in step (3) in the process and thus completing the assembly,

5) Finally, the outer surface of the assembly was smoothed by a fine grained emery paper.

3.4.1.10 Heater Positioning Rod

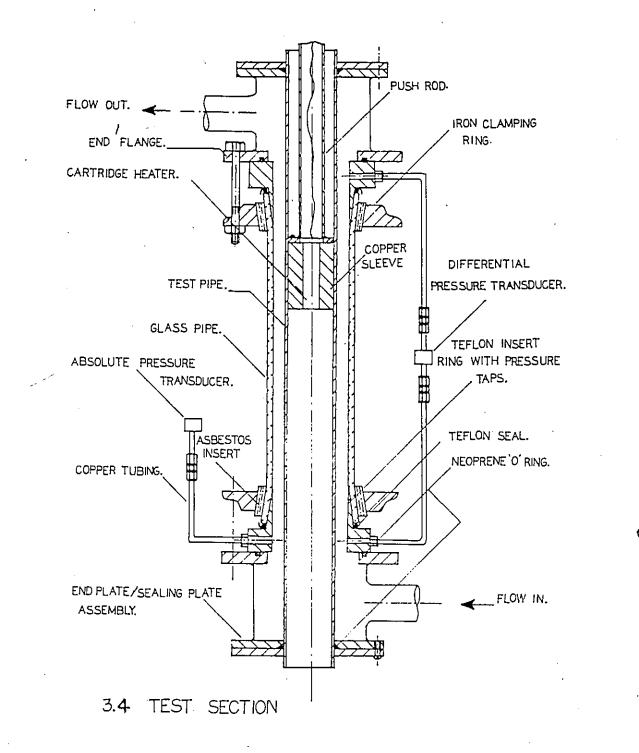
For positioning the heater/ sleeve assembly at any desired location a positioning rod mechanism was designed. To reduce the heat lost along this rod due to fin effects, stainless steel AISI(American Iron and Steel Institute) 316 (poor thermal conductivity) was selected. The end of the tube was welded to a flange, which in turn was bolted to the end of the sleeve.

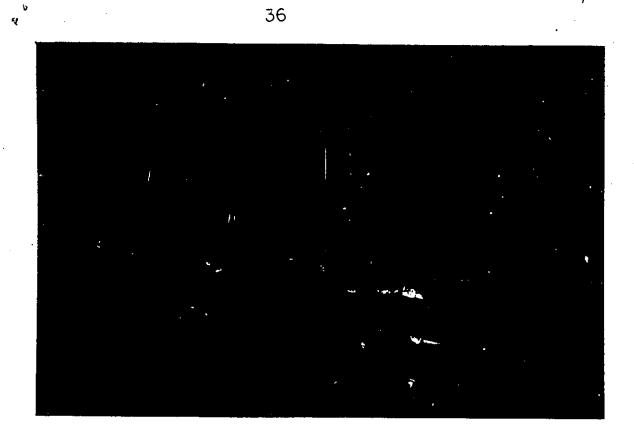
The heat lost through the push rod was estimated as 2.5 W,(assuming the rod as an infinitely long fin, and the rod loses heat to air whose temperature is an arithmetic mean of the wall and room temperatures) and the total heat lost from the flat ends of the sleeve was estimated as 0.8 W (assuming a laminar free convection around the flat ends) i.e., a total heat loss of 1.5% of maximum heat input. Since this heat loss is negligible, it was decided not to fill the test pipe internals with insulation. For heat loss calculations please refer Appendix-B.

3.4.1.11 Test Section Sealing Assembly

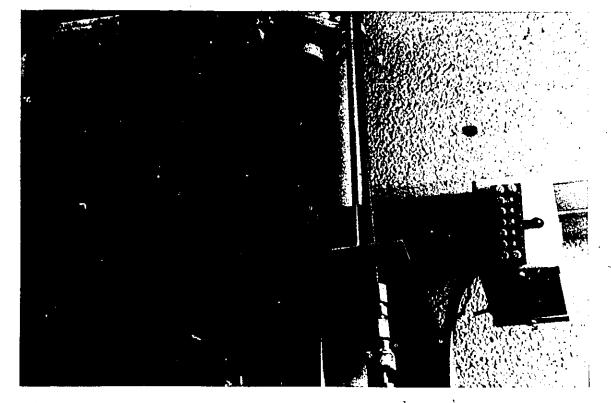
The test section is shown in Figure 3.4. The end caps used to seal each end of the glass annulus were constructed from an end flange made of free machining brass, an end plate/ sealing plate assembly made of free machining brass 11.11 mm (0.4375 in) thick, and a 38.1 mm (1.5 in) * 19.05 mm(0.75 in) unequal copper tee connecting them. The flow in/ out of the test section is through the tee branch. The end flange was 12 mm thick. Please refer to Appendix- C for flange design calculations.

The end flanges were bolted to the test section using a teflon





3.**5** a.



3**.5**ь

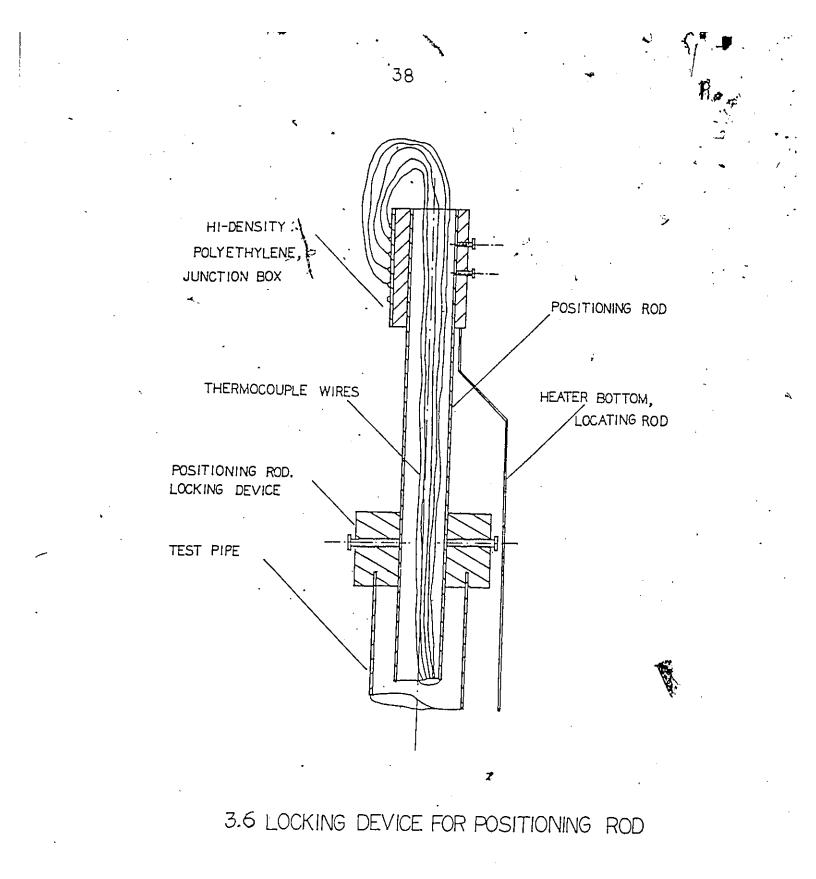
3.5 TEST SECTION ASSEMBLY

gasket ring and a teflon adapter piece to provide the glass to brass seal. As shown in Figure 3.4, the teflon adapter piece was profiled to be a companion for the flared ends in the glass section. Pressure measurement taps were machined in the shoulder of these adapters and are discussed in detail in Section 3.5.2. The teflon adapter piece/ end flange interface was sealed by a 41.275 mm (1.625 in) nominal diameter neoprene "0" ring which was seated in a sealing groove, in the end flange. The sealing groove was machined according to SAE J120a specifications[25] (Rubber Rings For Automotive Applications).

The test pipe was held in position with a 22.225 mm (0.875 in) nominal diameter neoprene "O" ring which was seated in a sealing groove cut into the end plate. The sealing groove was machined according to SAE J120a specifications [25]. As shown in Figure 3.4, the "O" ring is compressed against the end plate and the test pipe by a sealing plate which encircled the test pipe and is bolted to the end plate with four 3.175 mm(0.125 in) steel screws.

3.4.1.12 Locking Device For Positioning Rod

At the top of the test pipe is located the locking device, made from Hi-density polyethylene, for the heater/ sleeve assembly as shown in Figure 3.6. It has a 12.7 mm deep circumferential notch which fits snugly and is also glued to the test pipe using Omegabond 101 epoxy adhesive. The heater positioning tube can slide freely in the central hole. The positioning tube can be



Ģ

a

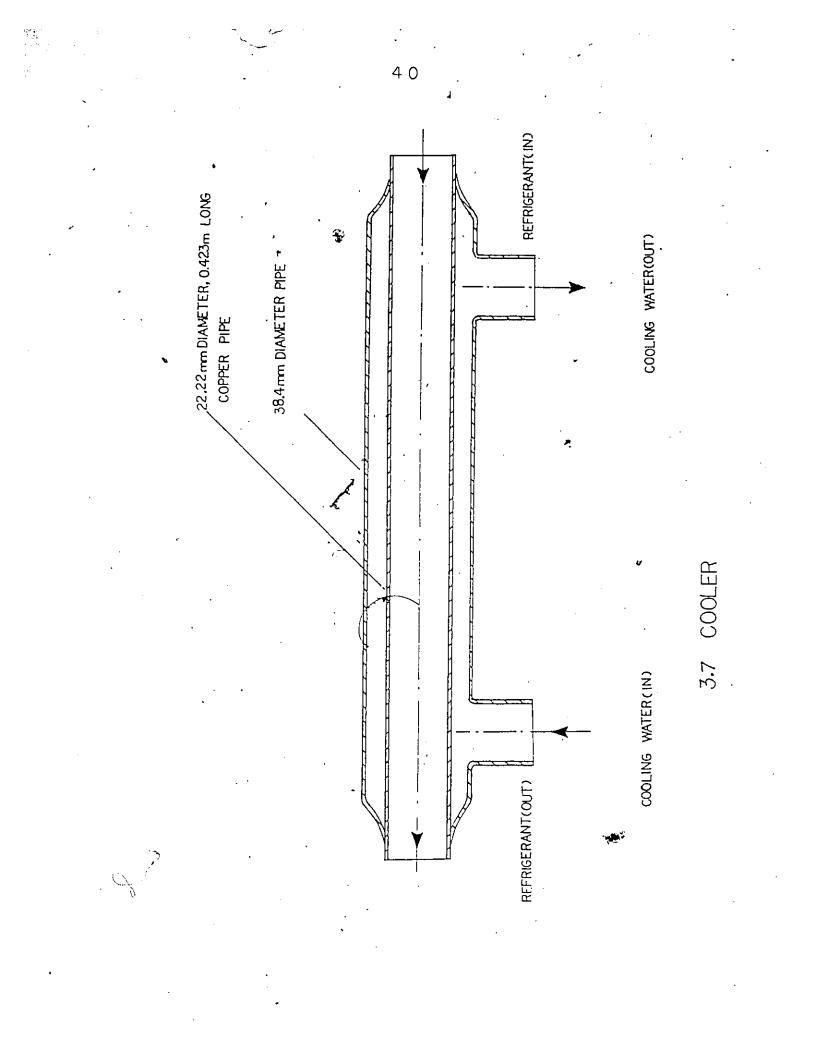
locked by two screws located diametrically opposite each other.

At the top of the positioning tube is a Fectangular junction box, for the five heater thermocouples as shown in Figure 3.6. A 3.175 mm diameter rod, parallel to the positioning tube and supported at the top from the junction box was mounted, for locating the heater bottom. The rod moved in tandem with the heater assembly. The four wall temperature measuring thermocouples were oriented in directions perpendicular to the side faces of the rectangular block.

3.4.2 Cooler

A cooler was installed to remove the energy added in the test section. It was decided that the cooler should be as close to the test section exit as physically possible, so that two phase pressure drop (if any) is reduced as far as possible. To avoid possible cavitation at the pump, the condenser elevation was set 1.68m above the pump. For ease of construction, it was decided that the cooler would be a double pipe (two coaxial pipes), counter flow heat exchanger as shown in Figure 3.7.

Water was selected as the cooling medium, since it has a low thermal resistance. For establishing a stable cooling flow rate at a constant temperature, a circulating Lauda constant temperature bath, type K-40, 115 V, 800 W, Messerate-Werk Lauda, W.Germany, was used.



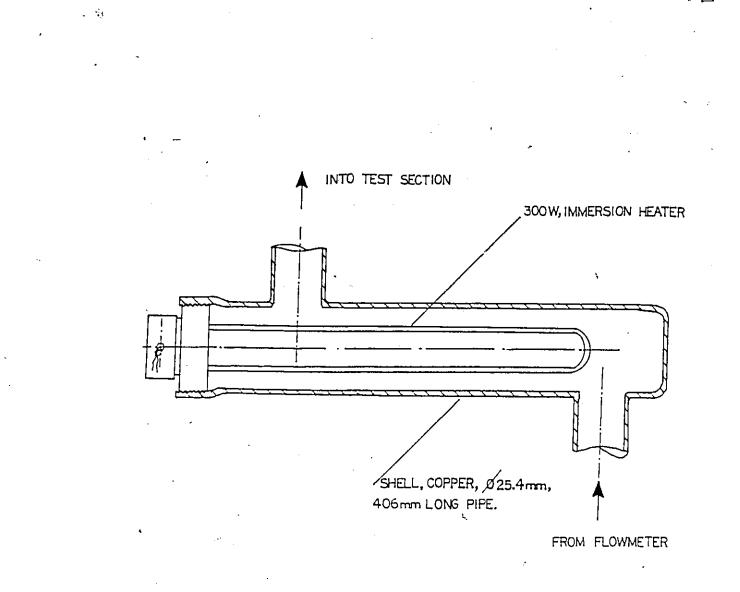
In sizing the cooler, the following extreme case was assumed with R-11 as the working fluid:

All of the fluid entering is saturated liquid and the maximum energy input in the main heater must be removed. The overall heat transfer coefficient , the effectiveness, flow ratio, NTU and finally, the heat transfer area were calculated. See Appendix-D, For details the cooler sizing.

The required area was found to be 0.04 m2 (0.56 m long, 22.225 mm outer diameter tube). However, a 0.61 length (10% over area) was provided for reasons of safety.

3.4.3 Preheater

The preheater is used to control the inlet fluid temperature in the test section. This unit, together with the system pressurizer, and the cooler, allows the experimentor to control both the inlet subcooling and the system pressure as parameters independent of each other. The cooler alone is capable of controlling the inlet fluid temperature, but since the voltage to the heater is easier to control than the coolant flow to the cooler, the preheater is included in the loop. The pressure drop in the preheater should be as small as possible, so that any chances of flashing or two phase boiling in the preheater are reduced. So, a horizontal configuration for the preheater was decided. Also, the power density of the preheater should be lower than the power density which will result in boiling. From [18], this was found to be



3.8 PREHEATER

5

÷

ĸ

35 kW/m2.

The preheater (refer to Figure 3.8) selected was steel sheathed TEMRO # 220 1968, 282.6 mm (11.125 in) long oil immersion heater with a rated output of 300 W at 120 V and a power density 31000 W/m2.

At a flow rate of 0.000315 m³/s (maximum flow the flowmeter is capable of measuring , refer to section 3.4.5), for R-11, the heater allowed the inlet temperature to be controlled within a range of 0 - 0.7° C, while at a minimum flow rate of 0.00315 m³/s (refer to section 3.4.5), this range was 0- 7° C.

The preheater end was a 19 mm (0.75 in) NPT male connection which mated with its counterpart in the preheater housing, which was built from a 25.4 mm copper pipe. The preheater was connected to a variable transformer capable of delivering 0-140 V. Since the power supplied to the preheater is not required for data reduction, a wattmeter was not connected.

3.4.4 System Pressurizer

The functions of the pressurizer unit are:

1) To maintain the system pressure at the desired level,

2) To dampen any pulsations caused by the pump,

3) To act as reservoir for the test fluid.

A commercially available bladder type pneumatic-hydraulic accumulator was found to meet all the above requirements. In order

that the system pressure be maintained constant, it is necessary that the volume of the gas charged bladder be approximately constant during the experimental run. That is, the change in volume of the gas bladder, due to volumetric changes in the loop because of vapour generation must be a minimum. Since we have subcooled flow boiling in the test section, we can be reasonably safe in assuming that the volume of vapour downstream of the main heater will be negligible. Hence, we can assume that the maximum volume of the vapour that can be generated in the test section corresponds to the volume of the heater length in the test section annulus and this was estimated as 0.00000905 m3.

The synthetic rubber partition material should have:

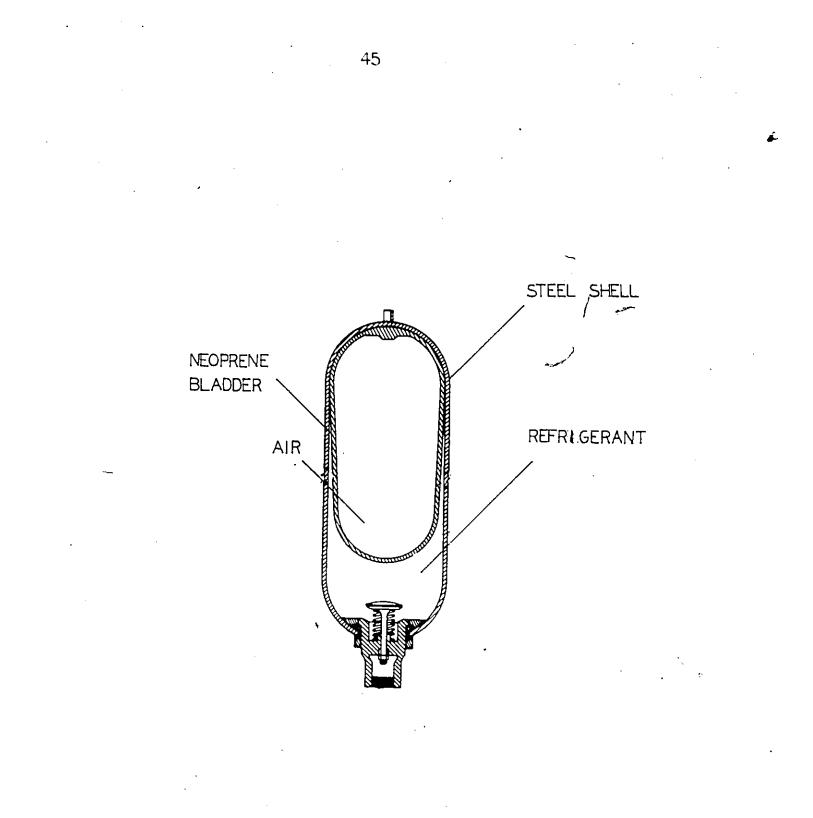
1) Tensile strength and heat resistance at the maximum design temperature,

52) Gas impermeability.

Pressurizer model # AB01B3T1A1K, refer to Figure 3.9, 0.000946 m3 size, 206.9 bars(3000 Psia) and Buna-N rubber bladder, supplied by Parker Fluid Power, Des Plaines, Illinois was found suitable and selected. The pneumatic pressure in the bladder in turn was controlled by a pressure regulating valve with a pressure indicator 0-12.05 bars (0-160 Psig) size.

3.4.5 Flowmeter

It was decided to use a variable area flowmeter for steady state flow measurements, because it was inexpensive, durable, stable,



3.9 SYSTEM PRESSURIZER

very reliable and does not require periodic calibration. The flowmeter should have the following characteristics:

1) It should be capable of withstanding the loop design pressure and temperature ,

It should be capable of providing the measurements accurately,
 The pressure drop encountered across the flowmeter should be small.

٢

A rotameter supplied by Omega Engineering Company, Stamford, Connecticut, model # FL-1504- A with borosilicate glass metering tube, SS 316 float, and Viton-A "O" ring , all compatible with R-11 and R-113, was selected. It could be operated at pressures up to 7.9 bars (100 Psig) and 121 degrees C (250 degrees F) with an accuracy of +/-2 % and repeatibility of +/-0.5 %. Its float had a design which made it virtually immune to viscosity variations. It was capable of measuring a flow range of 0.0000315 m3/s to 0.0.000315 m3/s for R-11 and 0.0000302 m3/s to 0.000302 m3/s for R-113 (corresponding to Reynolds number range of 2871 to 28710 for R-11 and 2475 to 24750 for R-113, in the test section evaluated at 20 degrees C). The manufacturer estimated that maximum pressure drop across the flow meter was 0.3302 m of water (13 in) (or 0.223 m of R-11 or 0.2189 m of R-113 , evaluated at 20 degrees C). The flow meter inlet and outlet were connected to the loop through 25.4 mm (1 in) NPT male connections. The manufacturer's calibration was based on water. The flowmeter was calibrated for R-11, by the following procedure:

The float position, the mass transferred and the time taken for this transfer was noted. The curve for R-11 was directly converted

from the manufacturer supplied curve for water, with the aid of the following formula:

$$Q_{fr} = \frac{Q_{w}}{\left[\frac{(\rho_{float} - \rho_{w}) \rho_{fr}}{(\rho_{float} - \rho_{fr}) \rho_{w}}\right]}$$

The calibration results are shown in Appendix-E and they matched within 6.4 % with the formula and hence it was decided to use the formula in the data acquisition program.

3.4.6 Loop Fittings And Piping

The various heat transfer and hydraulic components are made primarily of copper or brass. Loop piping is 19 mm (0.75 in) internal diameter , copper pipe and its corresponding fittings. The flow in the loop is controlled by a 19 mm (0.75 in) diameter ball valve. The loop was also provided with a hand operated, 9.525 mm (0.375 in) diaphram drain valve. A Schrader core valve 6.35 mm (0.25 in) was soldered downstream of this valve.

At the top-most point in the loop, a 6.35 mm liquid/ moisture indicator was installed. A hand operated 9.525 mm diaphram valve was soldered at the indicator downstream.

A filter drier, model ALCO ASD 45S6-VV was incorporated on the suction side of the pump to remove moisture and suspended particles (if any) in the loop.

A 0.000019 m³ volume, non condensable accumulator was soldered at the valve downstream. For sizing the accumulator, the loop volume was estimated. The pressure due to noncondensables at maximum achievable vacuum conditions was estimated. The amount of noncondensibles released is directly proportional to their gage pressure immediately before release into the atmosphere. Their final pressure was set at 5 bars gage (arbitarily) and using Boyles law, the volume of the accumulator was calculated. A Schrader core valve was soldered downstream of this vessel. The vent and drain Schrader valves were capped using a standard SAE threaded flare cap.

The section of the loop between the pump outlet and test section inlet was thermally insulated using a 12.5 mm thick , Armstrong, armflex insulation to minimize the heat losses to the ambient air. This is also a factor in obtaining thermal stabilization of the running system and will result in shorter waiting time for reaching steady state conditions.

3.4.7 Centrifugal Pump

The circulating pump is an important part of the forced convection loop and should have a steep Head-Flow characteristic, so that a small change in head does not produce flow oscillations. Positive displacement pumps have a flow proportional to speed and are almost independent of pressure differential. But they introduce large pulsations which can be detrimental to our studies on individual nucleation sites. So, it was decided to use a centrifugal pump with a steep Head-Flow characteristic. For sizing the pump, a tentative configuration was assumed for the loop and its various components and the pressure drop in the loop was calculated for a flow rate of $0.0003119 \text{ m}^3/\text{s}$, (Re = 28360 for R-11 and 24800 for R-113 evaluated at 20° C, in the test section). Please refer to Appendix-F for pressure drop calculations. In making these calculations, it was assumed that the two phase accelerational pressure drop component is negligible. This was justified because the two phase flow length was kept no longer than necessary and also because we have subcooled flow boiling, the void fraction is very small. The estimated pressure drop was 2.7 m and 2.8 m for R-11 and R-113-respectively at 20 degrees C.

If the pressure drop in the length between the cooler outlet and the pump inlet is less than the height of the downcomer pipe, we can be sure that the pump will not cavitate. The pressure drop was estimated as 0.371 m for R-11 and 0.385 m for R-113. Since the / height of the downcomer is 1.828 m, we have a minimum Net Positive Suction Head available at the pump inlet of 1.458 m. Centrifugal pump model #. J-7004-54 from Cole-Parmer Instrument Company, Chicago,Illinois was found to meet the requirements and was selected. For the characteristic curve of the pump, please refer to Appendix-G. The pump had a flow rate of 0.0003028 m3/s for R-11 and 0.0002996 m3/s for R-113 at the above estimated differential heads. This was as close to the desired flow rate as we could get. The pump required a Net Positive Suction Head of 0.1524 m (6in).The pump housing was Ryton, the spindle was ceramic and the

. 49

Ľ

sealing- "O" ring was Viton, all of which are compatible with both R-11 and R-113. The pump was coupled to a 0.04 HP, 3450 RPM, 115 V a.c motor through a sealless magnetic drive. The pump inlet and outlet were connected to the loop through 12.7 mm (0.5 in) NPT female connections.

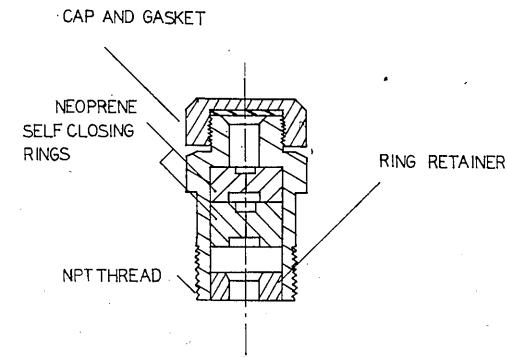
3.5 Instrumentation

Ì

3.5.1 Temperature Measurement

The wall temperature thermocouples have already been discussed in section 3.4.1.8. The refrigerant bulk temperatures at the inlet and the outlet to the test section were measured to control the heater settings; the outlet from cooler, and the cooling water bath temperatures were measured to control the cooling water flow rate; and the ambient temperatures was measured by 24 gage copper-constantan thermocouples with teflon insulation.

The thermocouples which measure the refrigerant bulk temperatures at the test section inlet and outlet, and the outlet from the cooler, were positioned with their tips held at the fluid stream centerline. The fittings holding these thermocouples is a self-sealing temperature test plugs model # OPNE-14 (refer to Figure 3.10) with two neoprene self-sealing rings, supplied by Omega Engineering Inc. The surface of the thermocouple is not cylindrical and there are possibilities of a leak. So, Superpoxee from Watsco Inc., Hialeah, Florida was applied over the thermocouple insulation to achieve an uniformly cylindrical surface. The sealing rings were punctured and the thermocouple



3.10 THERMOCOUPLE PLUGS

wire was threaded. The output from the thermocouples were fed into the scanner board of a 2240C Fluke data logger.

3.5.2 Pressure Measurement

To calculate the wall superheat, it is necessary to know the wall temperature and the local saturation temperature. Section 3.4.1.8 dealt with the instrumentation for wall temperature measurement. The inlet saturation temperature was **#**alculated by measuring system pressure and using thermodynamic correlations. The local saturation temperatures in the test section, were calculated by measuring the pressure drop in the test section and inlet pressure and calculated using thermodynamic correlations. The data acquisition software (see Section 3.5.3) performed r these calculations.

The system pressure and pressure drop in the test section was measured by piezoresistive pressure transducers. Model# PX 82-100 GV, 111.3 mV span, 7.9 bars (100 Psig) transducer was used for absolute pressure measurement and model# PX 83-005 DV, 143.9 mV span, 0.345 bars differential (5 Psid) transducer was used for bifferential pressure measurement. Both the transducers had an accuracy of +/- 0.25% of the full scale reading.

The power supply to these units was supplied by a constant current supply unit model# PS-KIT-1 which supplied 1.5 mA. This unit in turn received power through a 120 V/12 V stepdown transformer. The transducers and constant current supply unit were supplied by Omega Engineering Inc.

Two 3.175 mm (0.125 in) female NPT taps were machined in the shoulder of the bottom teflon adapter of the test section. One 4.76 mm (0.1875 in) female NPT tap was machined in the shoulder of the top teflon adapter piece. Care was taken to maintain the centre lines of the pressure taps perpendicular to the axis of the test section. All burrs around the holes were removed to eliminate any eddies which might cause a dynamic pressure component) in the measured static pressure. The absolute pressure transducer is connected to one bottom tap through 3.175 mm copper tubing and brass compression fitting. The differential pressure transducer is connected to the bottom tap through 3.175 mm copper tubing and brass compression fitting, and to the top through a 4.76 mm copper tubing and brass compression fitting.

The outputs from the pressure transducers was fed into the scanner board of a 2240C Fluke data logger. Corrections to the indicated pressures, due to elevation differences between the pressure tap and the transducer sensor was included in the data acquisition software.

ĩ

3.5.3 Data Acquisition System

A fast and convenient on-line data analysis was developed using a 2240 C Fluke data logger which was interfaced with a 64K Apple computer through a RS 232C serial card. The computer controlled

the data acquisition system. Please refer to Figure 3.11.

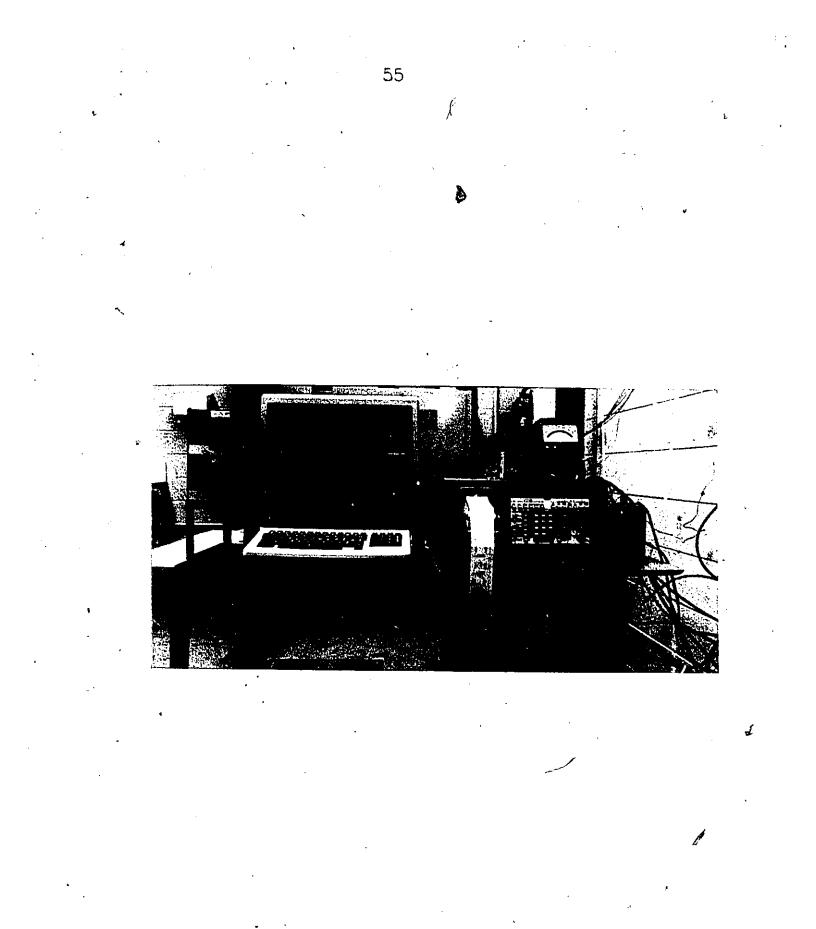
The computer data acquisition software "BOIL7" was written to enable fast collection of information on wall superheats, and heat transfer coefficients. The program was written in Apple Basic and was designed to ask clear, consise questions about the input data required for calculations. It is very user friendly and no prior knowledge of calculation methodology is required to run the program.

7

The sub-program titled "FLUKES.BJO" is a machine language program which enabled the Fluke's data transmission to be decoded and stored at specific memory addresses within the Apple computer. This program is automatically retrieved from disk storage to initialize the Fluke data logger whenever the data acquisition program "BOIL7" is run. Special thanks to Dr.N.W. Wilson for writing "FLUKES.BJO" software.

The computer was programmed to scan any number of times as directed by the experimentor. The data acquisition software used these scanned data, together with manually inputted data for atmospheric pressure, heater location, nucleation site location, flow meter reading, heater power, to calculate the wall superheats and heat transfer coefficients. The software allowed the experimentor to save the data results in a disk if he so desired.

Appendix- H describes the flow chart, the variables nomenclature, the program listing and a sample output. Note that in the flow



3.1) DATA ACQUISITION SYSTEM FOR THE EXPERIMENTAL SETUP

chart, unless otherwise indicated, a horizontal line indicates a flow from left to right, and a vertical line indicates a flow from top to bottom.

3.6 Loop Commissioning

3.6.1 Leakage Test

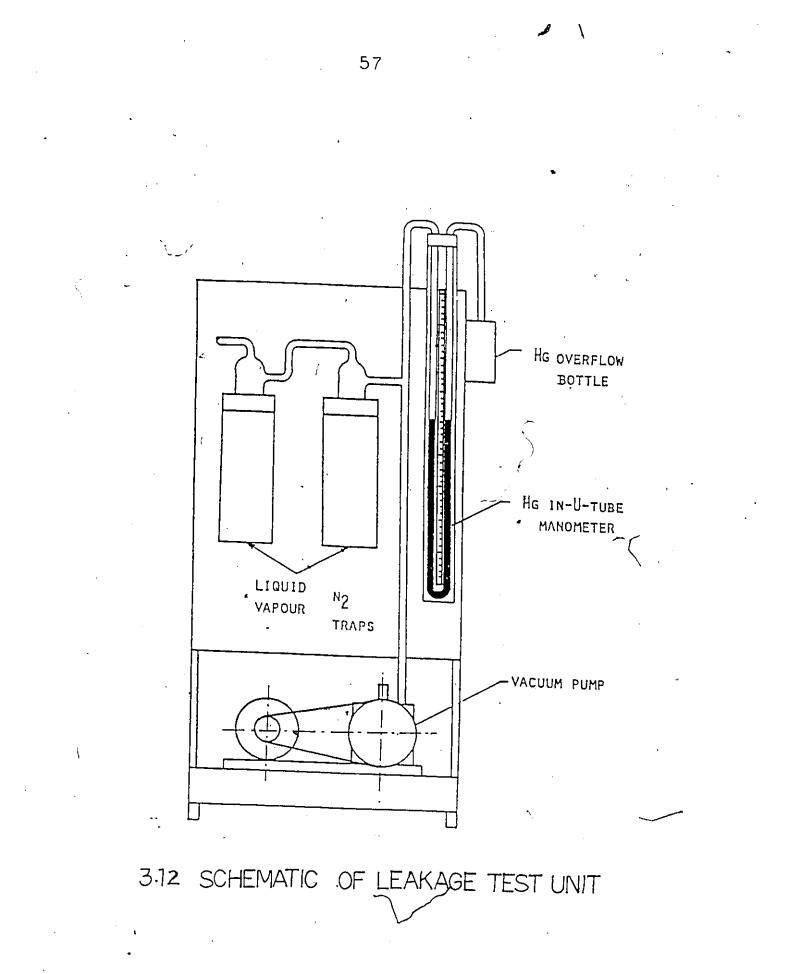
Leakage tests are necessary to prevent:

 Refrigerant loss to atmosphere (as in case of R-11),
 Moisture ingress into the system (as in the case of R-113), which will affect the results.

Three methods of leak detection were used as mentioned below: 1) The entire system was charged with air, to a pressure of 5.15 bars (60 Psig), and the system was isolated and the loop pressure was observed. A drop in indicated pressure indicates a leak, and the locations of the leaks was detected using a soap solution.

For ease of assembly, the loop was fabricated in sections, and was assembled through union joints. Numerous leaks were detected, especially in these unions and all attempts to tighten them were unsuccessful. These unions were replaced by brass compression fittings. Other leaks, depending on the nature of joints, were fixed using silver solder(for soldered joints) or Loctite sealant(threaded joints).

2) The system was evacuated to 744 mm of mercury using a vacuum pump system, shown in Figure 3.12. This unit was equipped with liquid_gas separators in series, and was immersed in liquid



nitrogen. This arrangement condensed the vapours in the loop. The vacuum was held by the system for thirty hours.

3) After the system was charged (as described in Section 3.6.2), the system was checked by a halogen electronic detector which is capable of detecting leaks of the order of 0.5 oz per year. The device emits a "beep" which increases in frequency when higher concentrations of halogens are sensed.

No leaks were found.

3.6.2 Charging Procedure

The following charging procedure was followed (refer to Figure 3.13):

1) The Schrader value in the loop vent was connected to the vacuum pump through a testing manifold provided with a gage.

2) The refrigerant charging cylinder was connected to the loop through a charging valve close to the cylinder, a charging hose and a Schrader valve in the filter drier. The cylinder was placed at an elevation of 1.5 m above the loop top most point to provide an additional hydrostatic head.

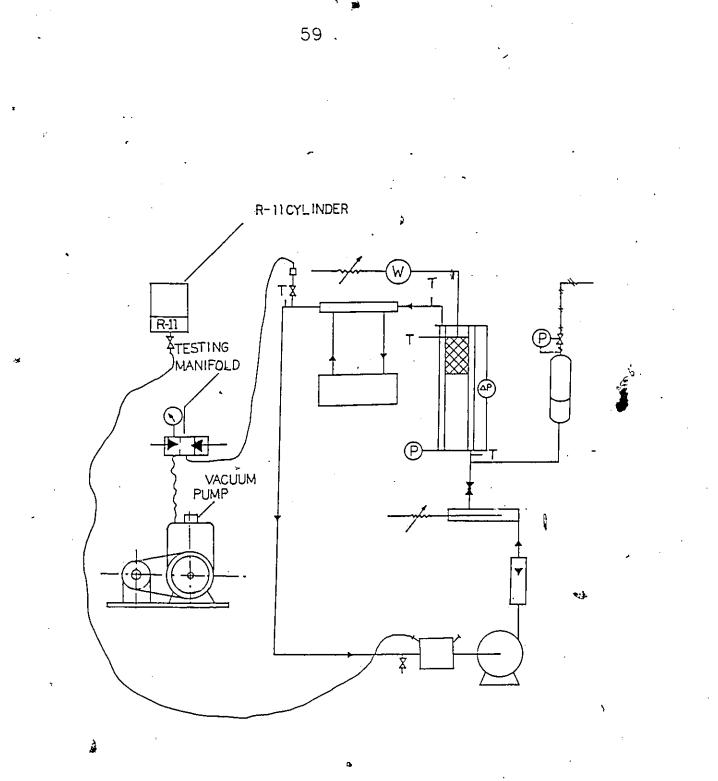
3) The system was charged by alternatively

(3.1) Opening the value in the vacuum line with the charging value closed, and pulling the desired vacuum.

(3.2) closing the value in the vacuum line with the charging value open, and charging the loop.

4) When the loop was completely filled as observed⁺ through the site glass in the top, the charging valve was closed.

5) The vent Schrader valve was depressed, until just a little



3.13 SCHEMATIC OF LOOP CHARGING FACILITY

liquid refrigerant from the system escaped. This way, we were sure that most of the noncondensibles in the loop were evacuated.

3.6.3 Results Of System Commissioning

The heat transfer loop was commissioned and the results are given

herewith :		•
Parameter	Targeted Range	Achieved Range
System pressure	1- 7.9 bars	2- 7.9 bars
Inlet subcooling	0-40°C;	0-75° C for R-11
		and 0- 105° C for R-113
		يف.
Reynolds number	3000-30000	2900-25000 for R-11
	`	and 2500-22000 for R-113,
		at 20°C
Heat flux at test 0-40000 W/m^2		0-60000 W/m ²
surface		
	•	• • •
Heater location	Anywhere along the	Anywhere along the
t	test section	test section
		· · · · ·

Bubble nucleation At all flow rates visualization

 \leq

Difficult to discern individual sites beyond Reynolds number 22000, for R-11

4. RESULTS, DISCUSSION AND CONCLUSIONS

4.1 Experimental Procedure

The following procedure was followed during the course of preliminary experimental runs:

1) The main heater was positioned at the desired location,

2) The loop was pressurized to test conditions,

3) The instrumentation was turned on, and the Fluke data logger was turned on and initialized. The computer was loaded with the data acquisition program "BOIL7",

4) The pump was turned on, and the throttling valve manipulated to achieve the required flow rate,

5) The preheater was adjusted to achieve the desired inlet subcooling, .

6) The main heater was turned on, and the input voltage was raised in small steps by manual control of the variac. The fluid exit temperature and test section wall temperatures were monitored,

7) Due to buoyancy effects, the flow rate changed, and it was adjusted if necessary,

8) The constant temperature, water circulation was turned on(if necessary) and the cooling water flow rate adjusted to maintain the subcooling at the test section inlet. The loop was now \mathcal{I} operating at a quasi-equilibrium condition that was suitable ferdata acquisition. The computer scans the temperatures and pressures and displays the wall temperatures, wall superheats and heat transfer coefficients. For comparison of results, the

nucleate boiling dormancy superheat predicted from Sato and

Matsumura's correlation was also displayed. Appendix-H gives a sample output of a scan.

9) Save the results if so desired, else, repeat the scan under the same conditions, or scan under new set of conditions,

10) The same procedure was followed for a decreasing heat flux.

The waiting time for the system to reach steady state conditions from "cold" startup was about 0.25 hours. Subsequent runs attained steady state in 0.15 hours. Twenty to thirty sets of readings were usually required for a complete cycle of increasing- anddecreasing heat flux.

Preliminary experiments were carried out for various heater power inputs, system pressures, inlet subcooling and fluid flow rates. These runs were trial runs to check the loop design and debug the data acquisition program.

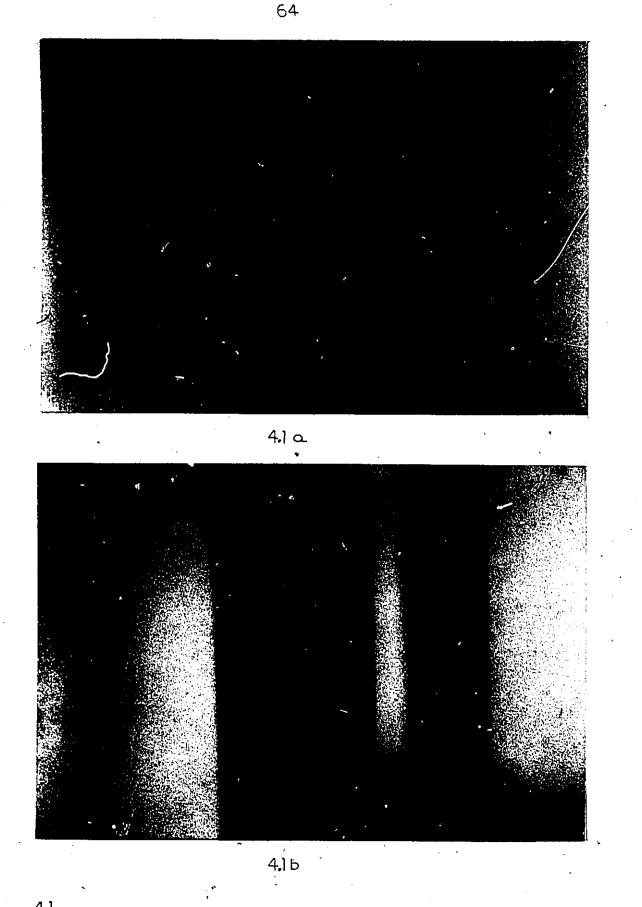
In a typical run, the inlet subcooling, system pressure and volumetric flow rate were held constant and the heater power was increased in steps, until nucleate boiling occured and was then decreased in steps, until the sites disappeared. Only the results, in which individual bubbles on the surface could be discerned were recorded. However, when the bubble population was large, the values were not used as incipience values. For observing these sites, a desk lamp was mounted and care was taken so that the heat from the lamp did not affect the results. The nucleation

sites were viewed through a convex magnifying lens. Figures 4.1 through 4.4 show the photographs of nucleation sites as captured by a low and high speed camera. They show the site behaviour at different boiling stages.

4.2 Results And Discussion

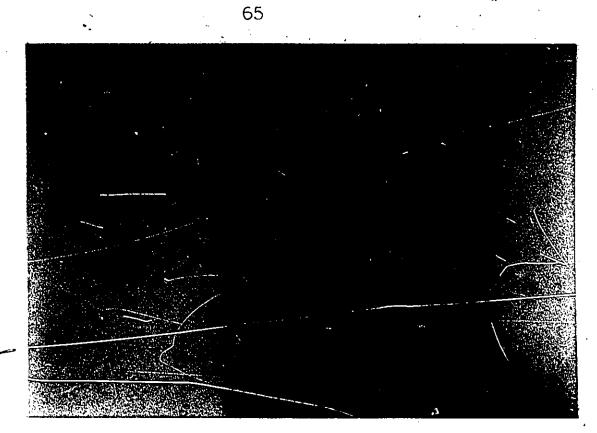
The experimental results are shown in Figures 4.5 through 4.7. These results are from [31]. The results presented are the local wall superheat at the topmost thermocouple elevation. In these figures, the surface heat flux has been shown as the dependent variable, though the wall heat flux is the experimentally controlled variable. This was done so that the results presented are consistent with typical boilding studies done in the past.

From Figures 4.5 and 4.6, we see that there is an abrupt drop in temperature after boiling inception. This temperature drop was about 25 degrees C, and a superheat of about 45 degrees C is required to initiate nucleation, under the test conditions. At about 48 degrees C, vigorous boiling erupted all over the test surface. This observed temperature drop of 25 degrees C, is higher than the results obtained by other researchers [11,12,13]. Also, note the hysteresis effects of the heat transfer coefficients. This hysteresis was obtained by cooling all sites, until they were quenched or made dormant. This is similar to the results observed in pool boiling by Corty and Foust [7] and Sabersky and Gates [9]. The sites were reheated, and we can observe the substantial difference in the behaviour of sites between the "cold" startup



4.] PHOTOGRAPH OF THE FLOW IN THE TEST SECTION

AFTER BUBBLE INITIATION

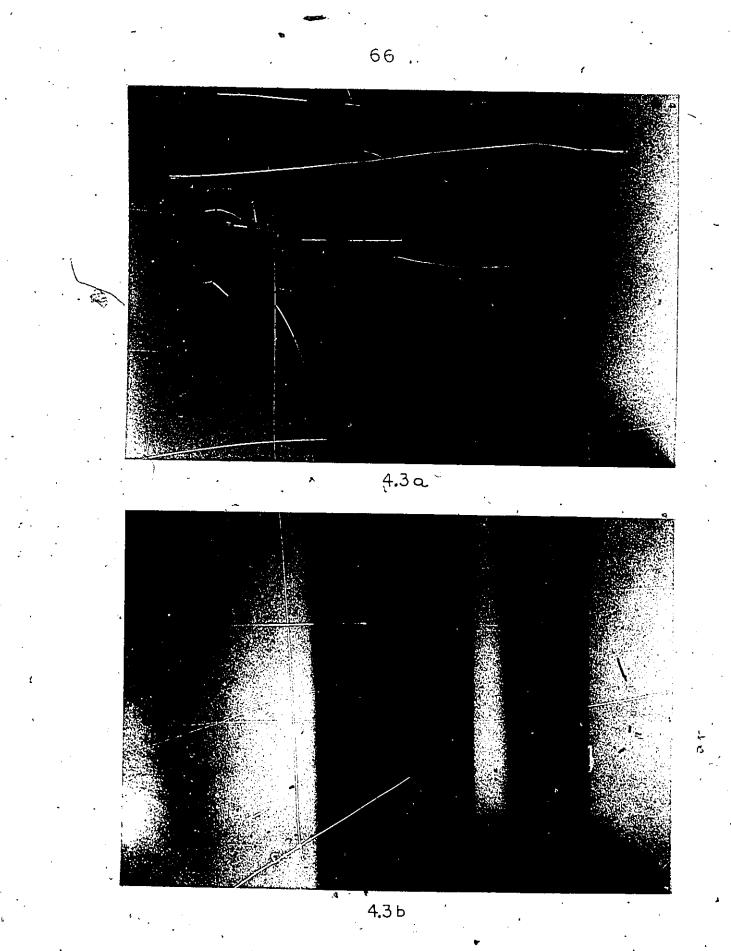


4.2 a.



4.2ь

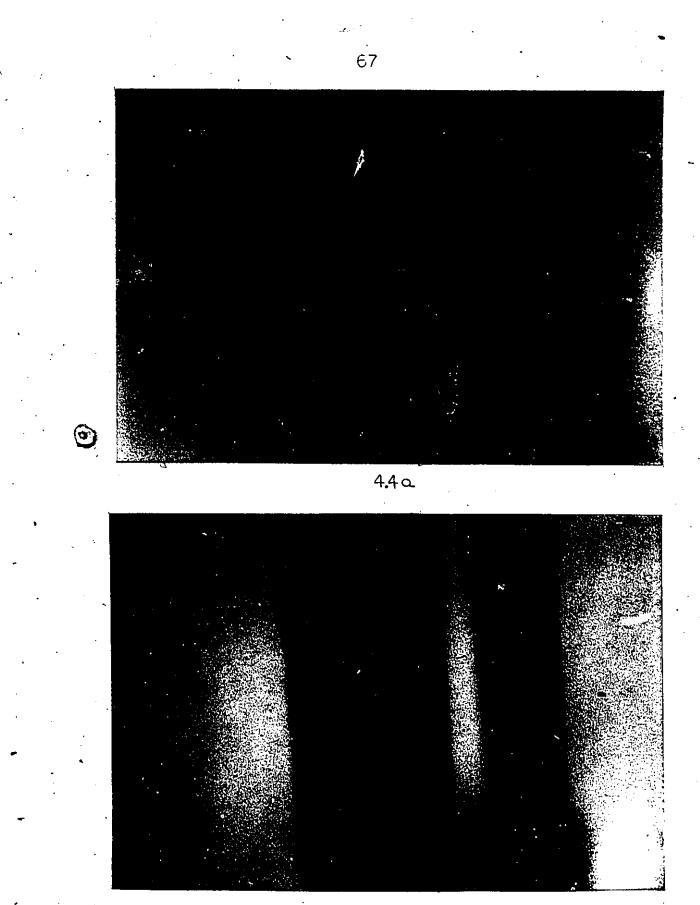
4.2 PHOTOGRAPH OF THE FLOW IN THE TEST SECTION SHOWING VIGOROUS SPONTANEOUS BOILING



4,3 PHOTOGRAPH OF THE FLOW IN TEST SECTION BEFORE DORMANCY

. U\

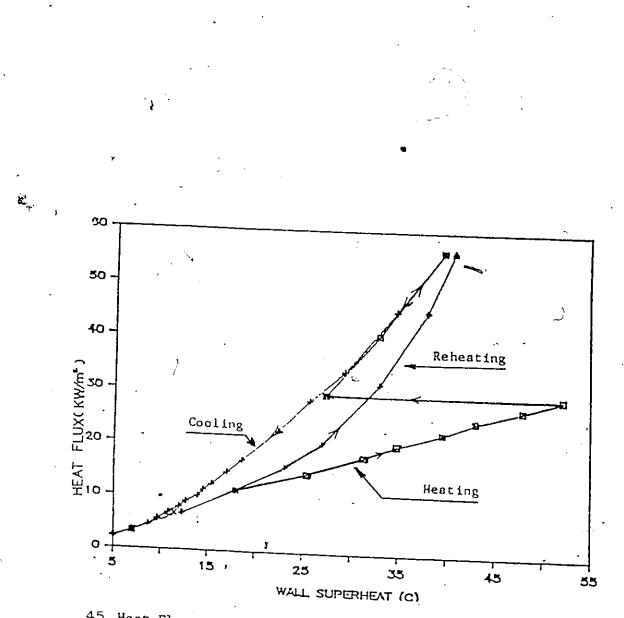
.

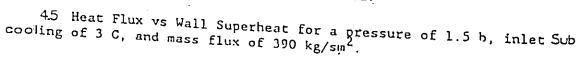


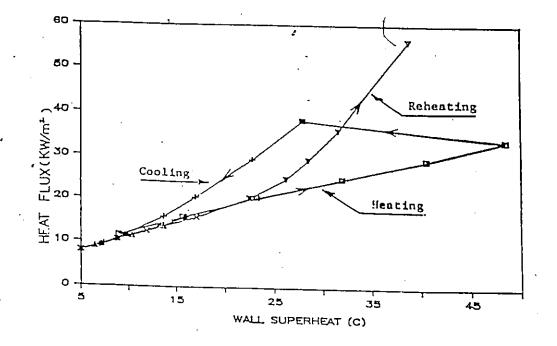
4<u>,</u>4 ь

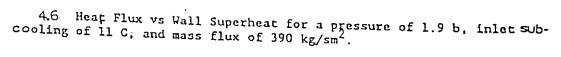
4.4 PHOTOGRAPH OF THE FLOW IN TEST SECTION SHOWING

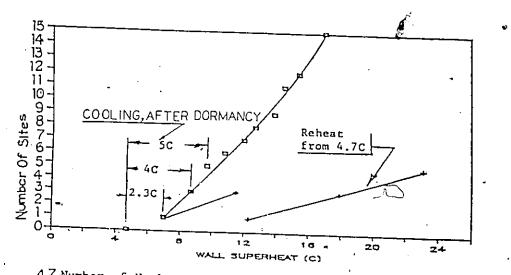
SMOOTHER TRANSITION TO VIGOROUS BOILING

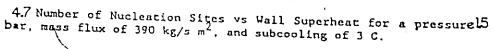












,

and the reheating process. In the second case, much higher heat transfer coefficients were achieved along with a smoother transition to vigorous boiling.

For the test at 1.9 bars, Figure 4.6, when the wall superheat wasdecreased to 6.8 degrees C all sites disappeared, and a number of

sites reappeared when the wall superheat was increased. Subsequently, when the wall superheat was reduced to 5 degrees C, one site reactivated, from its dormant state. When the wall superheat was reduced to 2 degrees C, the sites reactivated however , they behaved as though they were quenched, and dequired the same large wall superheat to initiate boiling from the "cold" startup. From Figures 4.5 and 4.6 we also infer that the inlet subcooling and system pressure affects the incipient wall superheat. This is similar to the results of Chen [10]. Also , we note that the temperature drop subsequent to boiling incipience is a function of subcooling and system pressure.

As shown in Figure 4.7, at a superheat of 9.6 degrees C, 5 sites were active, at 8.6 degrees C superheat, 3 sites were active and at 6.9 degrees C superheat, 1 site was active. When the superheat was reduced to 4.6 degrees C, none of the sites were quenched, but only made dormant. These same sites reactivated at wall superheats of 12, 18 and 23 degrees C as against 53 degrees C wall superheat required to initiate from "cold" startup. It was also observed that at maximum flow rates, it was not possible to discern individual nucleation sites.

4.3 Conclusion And Recommended Future Work

The design and commisioning of a forced convection heat transfer loop is reported for the study of:

1) the incipient boiling wall superheat,

2) the nucleate boiling quench wall superheat, and nucleate boiling dormancy superheat.

3) the hysteresis associated with the above phenomena for cycles of increasing followed by decreasing heat flux,4) the verification of the quench/ dormancy model.

Though there is a large volume of literature available, none has attempted to establish a quench/ dormancy model of nucleation sites in the incipient boiling region to explain the hysteresis effect. Hence, it was decided to build an experimental apparatus to gain a better understanding of above mentioned phenomena, so that mathematical models may be developed, which would aid us in predicting these phenomena.

The existing literature and mathematical models were reviewed in Chapter 2. The design, instrumentation and commissioning of the forced convection heat transfer loop was described in Chapter 3. Preliminary runs were carried out to check the loop design and debug the data acquisition program. It was found that the loop and its associated instrumentation is capable of studying the physical phenomena for which it was designed. Incipient boiling, quench superheats were measured, and their respective heat transfer coefficients evaluated. The hysteresis effect is very significant in this region. However, a major limitation of the present design is that it is not possible to observe individual sites at high flow rates.

Based on these results it is recommended that in the future, the following research be done:

1) Investigations should be carried out to study the phenomena for which the loop has been designed and the results compared with the existing correlations in the literature,

2) The results obtained should be used to develop a practical quench/ dormancy model to simulate hysteresis phenomena on a computer,

3) À comprehensive study of the pressure and temperature effects on boiling incipience needs to be performed.

4) Extend the applicability of experimental results, to a larger range of test section/ test fluid combinations. This might necessitate the upgrading of the main heater capacity.

An optical device should be used in conjunction with the photographic recording device to capture the first nucleation and quench event.

5) Finally, a time dependent model for the prediction of boiling

initiation and quench (given a certain pressure temperature history) be developed.

پ ۲

REFERENCES

1

5

1. Sato, T., and Matsumura, H.,<u>On The Conditions Of Incipient</u> <u>Subcooled-Boiling With Forced Convection</u>, Bulletin of JSME, <u>7</u>, # 36, pp 392-398, (1964).

2. Hsu, Y.Y., <u>On The Size Range Of Active Nucleation Cavities On A</u> <u>Heating Surface</u>, Transactions of ASME, Journal Of Heat Transfer, <u>84C</u>, 207, pp 207-216, (1962).

3. Han, C.Y., and Griffith, P., <u>The Mechanism Of Heat Transfer In</u> <u>Nucleate Pool Boiling - Part I(Bubble Initiation, Growth And</u> <u>Departure</u>), International Journal Of Heat And Mass Transfer, <u>8</u>, pp 887-904, (1965).

4. Howell, J.R., and Siegel, R., <u>Incipience</u>, <u>Growth</u>, <u>And</u> <u>Detachment Of Nucleating Bubbles In Saturated Water From</u> <u>Artificial Nucleation Sites Of Known Geometry And Size</u>, Proceedings of the third International Heat Transfer Conference, Chicago, 4, pp 12-21, (1966).

5. Bergles, A.E., and Dormar, Jr., T., <u>Subcooled Boilng Pressure</u> <u>Drop With Water At Low Pressure</u>, International Journal Of Heat and Mass Transfer, <u>12</u>, pp 459- 470, (1969).

6. Butterworth, D., Hewitt, G.F. (Editors), <u>Two-Phase Flow And</u> <u>Heat Transfer</u>, pg 134, pg 156, Oxford University Press, Oxford, (1977).

7. Corty, C., and Foust, A.S., <u>Surface Variables In Nucleate</u> <u>Boiling</u>, Chemical Engineering Progress Symposium ,<u>51</u>, Series 17, pp 1-12, (1955).

8. Bankoff, S.G., <u>The Prediction Of Surface Temperatures At</u> <u>Incipient Boiling</u>, Chemical Engineering Progress Symposium, <u>87</u>, Series 29, pp 87-94, (1959).

9. Sabersky, R.H., and Gates, C.W., <u>On The Start Of Nucleation In</u> <u>Boiling Heat Transfer</u>, Jet Propulsion, <u>25</u>, pp 67-70, (1955).

10. Chen, J.C., <u>Incipient Boiling Superheats In Liquid Metals</u>, Transactions of ASME, Series C, <u>90</u>, pp 303-312, (1968).

11. Abdelmessih, A.H., Fakri, A., and Yin, S.T., <u>Hysteresis Effects</u> <u>In Incipient Boiling Superheat Of Freon-11</u>, Proceedings of Fifth International Heat Transfer Conference, <u>4</u>, pp 165-169, (1974).

12. Joudi, K.A., and James, D.D., <u>Incipient Boiling</u> <u>Characteristics At Atmospheric And Subatmospheric Pressures</u>, Transactions of ASME, Journal of Heat Transfer, Series C,<u>99</u>, pp 398-403, (1977). 13. Stauder, F.A., and McDonald, T.W., <u>Experimental Study Of A</u> <u>Two-Phase Thermosiphon Loop Heat Exchanger</u>, ASHRAE Transactions, <u>92</u>, Part 2, pp 486-493, (1986).

14. Ge, D., McDonald, T.W., and Mathur, G.D., <u>Hysteresis In Two-</u> <u>Phase Thermosiphon Loop Heat Exchangers</u>, ASHRAE Transactions, <u>93</u>, Part 2, pp 2754281, (1987).

15. Bergles, A.E., and Rohsenow, W.M., <u>The Determination Of Forced</u> <u>Convection Surface Boiling Heat Transfer</u>, Transactions of ASME, Journal of Heat Transfer, Series C, <u>365</u>, (1964).

16. Davis, E.J., and Anderson, G.H., <u>The Incipience Of Nucleate</u> <u>Boiling Forced Convection Flow</u>, AIChE Journal,<u>12</u>, #4, pp 774-780, (1966).

17. Hino, R., and Ueda, T.,<u>Studies On Heat Transfer And Flow</u> <u>Characteristics In Subcooled Flow Boiling-Part 1. Boiling</u> <u>Characteristics</u>, International Journal Of Multiphase Flow,<u>11</u>, #3, pp 269-281, (1985).

18. <u>Industrial Electric Heaters For Liquids And Gases</u>, Chromalox Canada, Rexdale, Ontario, CCSL-300-8, pg-34, (1986).

19. Kakac, S., and Veziroglu, T.N., <u>Two-Phase Flows And Heat</u> <u>Transfer</u>, Volume 2, pp 623-645, pp 747-766, Hemisphere Publishing Corporation, Washington, (1977).

20. Hwang, K.S., <u>Two Phase Thermosiphon Loops-Part I.</u> (An <u>Experimental Study Of A 3/8 in Diameter 2 Ft*4 Ft Loop</u>, M.A.Sc. Thesis, University Of Windsor, Windsor, Ontario, (1976).

21. Kays, W.M.,<u>Convective Heat And Mass Transfer</u>, pp 194-196, McGraw-Hill Book Company, New York, (1966).

22. Ruffel, H.H., Editor, <u>Machinery's Handbook</u>, pp 1517-1525, Industrial Press Inc., New York, (1987).

23.<u>Temperature Handbook</u>, Nanmac Corporation, pg L-35, Framingham Court, Massachusetts, (1985).

24. Chapman, A.J., <u>Heat Transfer</u>, pp 360-368, The Macmillan Company, New York, (1967).

25.<u>SAE Handbook</u>, Volume 1, pp 11.131-11.137, Society Of Automotive Engineers, Warrendale, Fennsylvania, (1988).

26.<u>ASHRAE Handbook, Fundamentals</u>, pp 16.1-17.19, American Society Of Heating, Refrigerating And Air-Conditioning Engineers, Inc., Atlanta, Georgia, (1985).

27. Ludwig, E.E., <u>Applier Process Design For Chemical And</u> <u>Petrochemical Plants</u>, Volume 1, pp 45-125, Gulf Publishing Company, Houston, Texas, (1964).

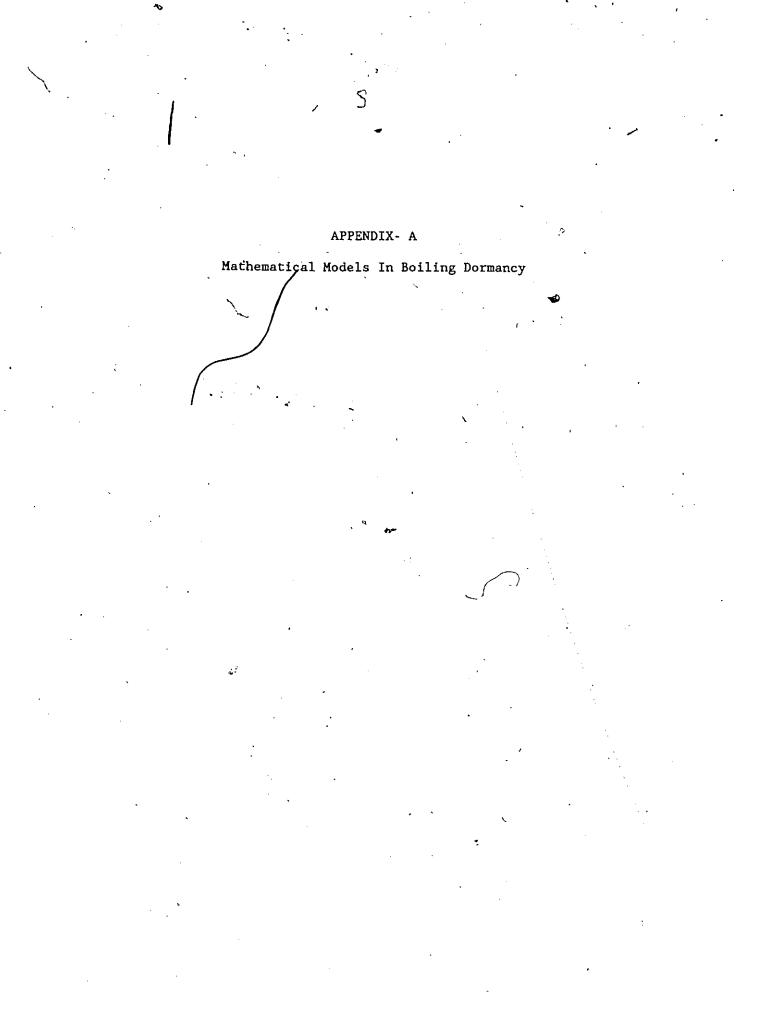
28. Ludwig, E.E., <u>Applied Process Design For Chemical And</u> <u>Petrochemical Plants</u>, Volume 3, pp 1-98, Gulf Publishing Company, Houston, Texas, (1964).

29. Brownell, L.E., and Young, E.H., <u>Process Equipment Design</u>, pp 219-250, Wiley Eastern Limited, New Delhi, India, (1983).

30. Bergles, A.E., Bakru, N., and Shires, J.W. <u>Cooling Of High-Power-Density Computer Components</u>, M.I.T. Engineering Projects Laboratory Report # DSR 70712-60 (1968) from cross reference, Murphy, R.W., and Bergles, A.E., <u>Subcooled Flow Boiling Of Flurocarbons-Hysteresis And Dissolved Gas Effects On Heat Transfer</u>, Proceedings Of The 1972 Heat Transfer And Fluid Mechanics Institute, pp 408-409, Stanford University Press, Stanford, California, (1972).

31. McDonald, T.W., and Shivprasad, D.,<u>Incipient Nucleate Boiling</u> <u>And Quench Study</u>, CLIMA 2000-, Proceedings of Second World Congress on Heating, Ventillation, Refrigeration and Air, Conditioning, (1989).

ు



semi-sphere, we have from Helmholtz's equation,

For thermal equilibrium,

 $P_{v} - P_{f} = \frac{2 \sigma}{r} - (A4)$

 $T_v = T_f$ at $y = \lambda r_c - - (A5)$

:

Bergles and Rohsenow assume $\lambda-1$; Hsu recognises it as a function of contact angle and cavity geometry, but suggests a typical value of 2.

Since P > P, and the vapour is at saturation temperature corresponding to its pressure, the surrounding liquid must be superheated with respect to its pressure. This superheat is related to its pressure by the Crausius-Clapeyron equation

 $\frac{dP}{dT} \frac{f_{g}}{\nu T} - - (A6)$ Considering the vapour as a perfect gas, and eliminating ν , we have,

$$\frac{dP}{dT} \frac{h}{r_{g}} \frac{P}{P} \frac{r^{2}}{r^{2}} - - (A7)$$

Assuming there is no variation in h_{fg} within the temperature limits in which we intend integrating, and integrating equation (A7) between limits T_{μ} , P_{μ} and T_{ν} , P_{ν} , we have,

)

$$T_{v} - T_{s} = \frac{RT_{s}T_{v} \ln (1 + 2\sigma / r_{cs}^{P})}{\frac{h_{rg}}{h_{rg}}} - - (A8)$$

Since, $2\sigma/r_{cs}^{P} \ll 1$, $\ln (1 + 2\sigma/r_{cs}^{P}) \doteq 2\sigma/r_{cs}^{P}$. Equation (A8) can be put in general as,

 $T_v = T_s (1 + A/r_c) ---(A9)$

Equations (A2) and (A9) are shown in Figure A.1.

semi-sphere, we have from Helmholtz's equation,

$$P_{v} - P_{f} = \frac{2 \sigma}{r_{c}} - - (A4)$$

For thermal equilibrium,

$$T_v = T_f$$
 at $y = \lambda r_c - -- (A5)$

Bergles and Rohsenow assume λ -1; Hsu recognises it as a function of contact angle and cavity geometry, but suggests a typical value of 2.

Since $P > P_{f}$, and the vapour is at saturation temperature corresponding to its pressure, the surrounding liquid must be superheated with respect to its pressure. This superheat is related to its pressure by the Clausius-Clapeyron equation

$$\frac{dP}{dT} \frac{h}{vT} - - (A6)$$

Considering the vapour as a perfect gas, and eliminating v, we have,

$$\frac{dP}{dT} \frac{h}{r_{B}} \frac{P}{r_{B}} - - (A7)$$

Assuming there is no variation in h_{g} within the temperature limits in which we intend integrating, and integrating equation (A7) between limits T, P and T, P, we have,

$$T - T = \frac{RT T}{s} \ln (1 + 2\sigma / r P)$$

$$\frac{h_{fg}}{h_{fg}} - -(A8)$$

Since, $2\sigma/r_c P_s \ll 1$, ln $(1 + 2\sigma/r_c P_s) \doteq 2\sigma/r_c P_s$. Equation (A8) can be put in general as,

 $T_v = T_s (1 + A/r_c) --- (A9)$

Equations (A2) and (A9) are shown in Figure A.1.

For a given fluid, given flow rate, bulk fluid temperature, heat transfer coefficient are fixed. This in turn fixes the intercept of fluid temperature profile with $T = T_{bulk}$ line.

The variables in equations (A2) and (A9) are T_{w} , q and r_{c} . The

fluid temperature profile is fixed by either fixing T_w or q When equation (A2) is tangent to equation (A9), the conditions correspond to nucleate boiling For $q > q_{dormancy}$, two values of r_c are obtained. Cavities lying outside the range of those two solutions are ineffective dormancy sites, while those lying in the range are effective, but not necessarily active sites. For incipient nucleate boiling dormancy,

$$T_{E}(1+A/r_{c}) = T_{b} + \frac{q}{h} - \frac{\lambda q}{k} r_{c}$$
or
$$\frac{q}{k} \lambda r_{c}^{2} r_{c}(\Delta T_{aub} - q / h) + AT_{a} = 0 - - - (A11)$$

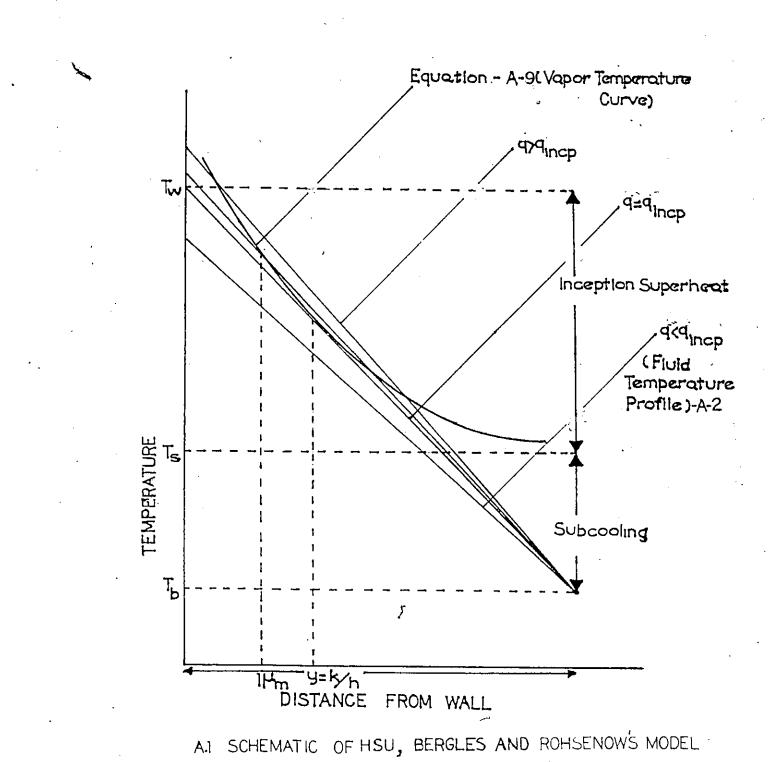
È.

Equation (A-11) is a quadratic in r_c , and for incipient dormancy, we must have equal roots.

$$(\Delta T_{aub} - q / h)^2 - 4 q \lambda A T_{aub} - --(A12)$$

Equation (A-12) is a quadratic in q, which results in two roots. The root with the negative sign corresponds to the solution in the third quadrant, where $T_{w} < T_{b}$, and therefore has no physical significance.

$$q = h \begin{bmatrix} \Delta T_{sub} + \frac{2\lambda T_{shA}}{k} + \begin{bmatrix} \Delta T_{sub} + \lambda hAT_{s} \\ k \end{bmatrix} \begin{bmatrix} 4\lambda T_{shA} \\ k \end{bmatrix} \begin{bmatrix} 0.5 \\ k \end{bmatrix} - (A \ 13)$$



The sum of second and third terms in equation (A 13) gives the value of $(T_{w}^{-}-T_{b}^{-})$ necessary for incipient nucleate boiling dormancy, where

 λ -1; A = $\frac{2\sigma}{1.25\rho_{g}h_{fg}}$ (Bergles and Rohsenow's model) and λ = 2; A = $\frac{2\sigma}{\rho_{g}h_{fg}}$ (Hsu'smodel) $\rho_{g}h_{fg}$

2 e



Heat Losses Through The Push Rod and Sleeve End Faces Calculations

١,

APPENDIX-B

The heat lost from the push rod and the flat ends of the sleeve is presented in this section. These calculations were done to make a decision, if the inside of the test pipe should be filled with insulation to minimize the heat losses.

B.1 Heat Lost Through The Push Rod

Assumptions:

1. The rod is infinitely long.

2. The temperature of air is an arithmetic mean of heated wall and room temperature.

Temperature of wall during inception $-115^{\circ}C + 18^{\circ}C - 133^{\circ}C$.

Room temperature \div 21°C.

. Mean temperature - $(133 + 21)/2 - 77^{\circ}C$.

Air properties at 77°C;

 $\rho = 0.9950 \text{ kg/m}^3$

 $\mu = 208.2 \times 10^{-7} \text{ N} \cdot \text{s/m}^2$

 $\beta = 1/350 \ ^{\circ} \text{K}^{-1}$

length of the push rod - 0.60975 m.-1

Temperature difference between the heated wall temperature and ambient air - $\Delta T = 112^{\circ}C$.

Pr = 0.70

$$g = \int_{a}^{1} (2 + 3) g = g = \frac{1}{a^2}$$

$$G = -\frac{1^2 a^2}{a^2} = \int_{a}^{a} (2 + 3)$$

. h_{air} = 2.36 Btu/hr ft^{2o}F = 13.397 W/m² C. . $q_{\text{lost from 1 flat aide}} = h_{\text{air}} A_{\text{x}} \Delta T$

 $-13.397 \times \Pi_{4} * (0.000402644 - 0.000062802)^{0.5} \times 112$

-0.4 W.

. . q_{lost from 2 flat sides} - 0.8 W.

. Total heat lost from the sleeve and the push rod - 3.3 W.

- 1.5 % of maximum heat input.

Since this is negligible, it was decided not to fill the inside of the test pipe with insulation.

á

APPENDIX - C

.

٢.

End Flange Design Calculations

. .

APPENDIX-C

This section presents the design of the end flange of the test section as in [29]. For ease of welding the test section inlet and outlet copper tees, and also for ease of machining, a brass flange was chosen. Since brass flanges are not off the shelf items, they had to be designed specifically for our requirements. Since the units in graphs in [29] are British, the same has been retained here.

1.Since the operating pressure < 300 Psi, and operating temperature $< 700^{\circ}$ F, a ring type flange (loose flange) was chosen.

2. Bolt material :BS 3692 , tensile strength - 65250 Psi.

3. Allowable bolt stress - 65250/4 - 16312.5 Psi.

4. Bolt area(M8 bolt) - $\frac{\Pi(8/25.4)^2}{4}$ - 0.2474 in²

5. Maximum bolt load - (16312.5)(0.2474) - 4035.7125 lb

6. Bolt circle diameter - 2.8 in,

7. Gasket centre circle diameter -(gasket 0.D + gasket I.D) 2

-(1.062+1.65)/2-1.356 in.

8. Moment on flange under no load conditions-

(4035.7125)(2.8-1.356)

2

9. f for brass - 81000/4 - 20250 Psi.

10. Outside diameter of flange - 2.8 in.

11. Inside diameter of flange - 1.375 in. Therefore, the ratio of

diameters = $\Omega = 2.8/1.375 = 2.036$.

12. Y (factor involving
$$\Omega$$
) = 0.66845 +5.7169($\log_{10}\Omega$) Ω^2
 $\Omega^2 - 1$ = 2.34

\

13. Flange thickness $-\left[\frac{Y (Moment maximum)}{f B}\right] = 0.4797$ in.

١

- 12.18 mm.

APPENDIX - D

COOLER DESIGN CALCULATIONS

APPENDIX-D_

COOLER DESIGN [28]

ŕ

Assuming That All The Fluid Coming In Is Liquid

1. Heat to be removed - 225 - p

2. Recommended water velocity - 0.610- 0.915 m/s and 0.610 m/s was chosen.

3. Inlet water temperature - 15°C.

4. ΔT for water in the cooler = 0.2° C. (arbitarily chosen value)

5. Mass flow rate of water in the cooler

 $\dot{m}_{w} = p/C_{p} \Delta T = \frac{225}{4186(0.2)} = 0.250 \text{ kg/s}.$

.'. Volumetric flow rate of water - Q - 0.00025 m^3/s .

6. . . . crossectional area of the water flow area = Q/u0.000250/0.610 = 0.0004098 m² = 4.10 cm².

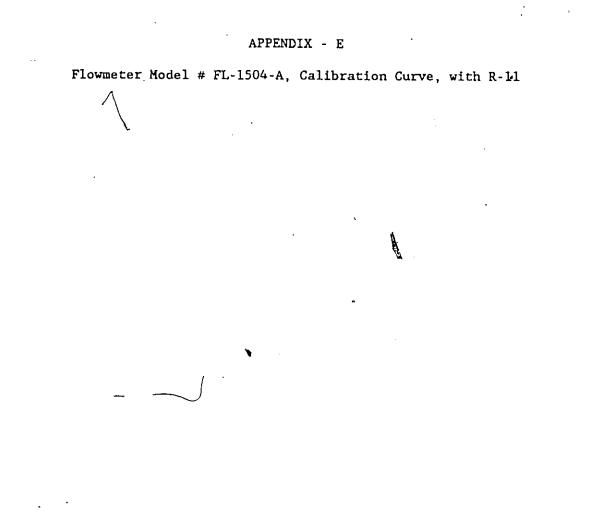
i.e., $4.1 - \frac{\Pi (D_0^2 - 2.2225^2)}{4}$. Hence, a 31.75mm inside 38.1 mm outside diameter pipe was chosen. 7. Calculation of overall heat transfer coefficient $Nu_{Refrigerant side} = 0.0296 \text{ Re}^{0.8} \text{ Pr}^{0.333}$ Pr = 4.2147 $Re_{minimum} = 7100$ $\therefore Nu = 57.62 = \frac{h_{inner side}}{k}$ $\therefore h_{inner side} = (57.62)(0.07793)/0.0201 = 223.38 \text{ W/m}^2 \text{ C}$

Similarly, Re = 5570 and Pr = 5.83 . Nu - 52 87 . h = $(52.87)(.613)/0.022225 = 1458.23 \text{ W/m}^2 \text{ C}$. . . $K_{copper} - 401 \text{ W/m K}$ Thickness of copper pipe - 0.002125 m .'. U = 193.36 W/m² C 8. Calculation of effectiveness Temperature of refrigerant (saturation at 2 bars)- 45° C $\cdot \cdot \cdot p_{\text{maximum}} = (0.0003119)(1480)(0.907)(45-15) = 12600 \text{ W}$ $\therefore \epsilon = 225/12600 = 0.0179$ 9. Calculation of R R-11 R-113 Maximum $\dot{m}C_{p} = 0.418 \text{ kJ/s } C_{p}$ 0.497 kJ/s C Minimum $\dot{m}C_{p}$ = 0.0418 kJ/s C 0.0497 kJ/s C mC_p for water - 1.0465 kJ/s C. Since $(\dot{m}C_p)_{hot} < (\dot{m}C_p)_{cold}$ R-(mCp) hot - 0.04 (mC_p) 10 Calculation of NTU NTU - $-\frac{1}{R-1}$ ln $\begin{bmatrix} \epsilon & -1 \\ \epsilon & R-1 \end{bmatrix}$ ¹ - 0.018 .'. L - NTU(m C) υпр

- 93

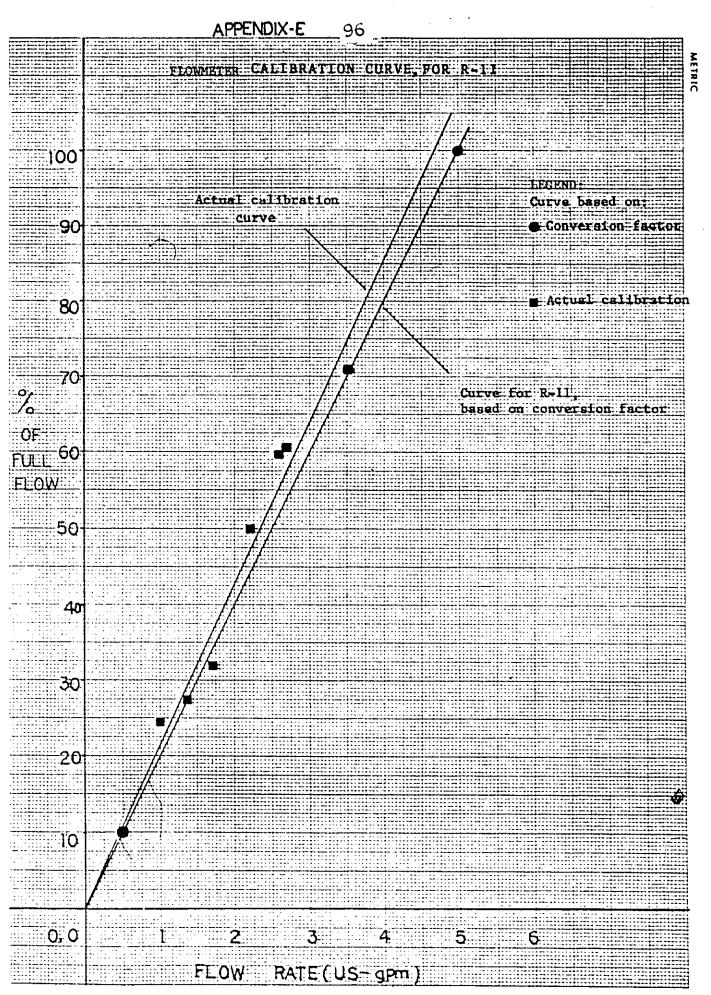
- 0,56 m

However, 0.61 m length (10% over area) was provided for reasons of safety.



ð

ł

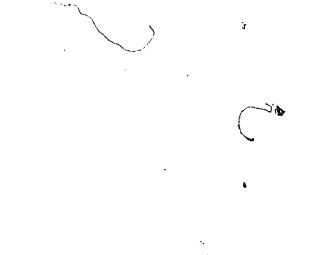


. .

APPENDIX-F

Loop Pressure Drop Calculations







APPENDIX - F

.....

ţ

F.1 Pressure Drop In The Test Loop Calculations	
Note that in these calculations, all the fl	luid properties are
evaluated at 20° C.	Ø
F.1.1 Equivalent Length Calculations.(19 m	m diameter pipe,
equivalent lengths are calculated according to [27].)	
DESCRIPTION	LENT LENGTH (m)
1. Straight pipe (outlet from pump)	0.4572
2. Standard tee (inlet to preheater)	1.3106
3. Straight pipe (preheater shell)	0.2286
4. Standard tee (outlet from preheater) 🧳	1.3106
5. Globe valve	5.4864
6. Standard 90° elbow	0.5334
7. Straight pipe	0.2286
8. Standard tee (inlet to test section)	1.3106
9. Standard tee (outlet from test section)	1.3106
10 Straight pipe (heat exchanger)	1.4478
11.Standard 90° elbow	0.5334
12. Straight pipe (down comer)	1.8228
13. Standard 90° elbow	0.5334
14. Straight pipe (leading to pump suction)	1.7526
15. Standard 90° elbow	0.5334
16. Standard 90° elbow	- 0.5334
17. Sudden expansion (strainer inlet $d/D = 1/4$) 0.5334 *

98

÷

18. Suden contraction (strainer outlet d/D - 1/4) 0.2591 \sum Equivalent length (m)(excluding the test section) - <u>19.909</u>

F.1.2 Pressure Drop In The Pipe (Excluding the test section) Area of cross section of pipe = $\frac{\Pi (0.01905)^2}{4}$ = 0.0002851 m² Flow rate (minimum) = 0.4933 gpm (US)=0.000031119 m³/s Flow rate (maximum) = 4.933 gpm (US)= 0.00031119 m³/s . . . G (minimum, R-11) = $Q_{min}\rho = \frac{(0.000031119)(1480)}{0.0002851}$ = 161.5507 kg/s m² and G (maximum, R-11) = 1615.507 kg/s m²

Similarly, for G (minimum, R-113) - $\frac{(0.000031119)(1480)}{0.0002851}$ - 164.6102 kg/s m²

. Reynolds number (minimum, R-11) - $\frac{G}{\mu}$ - (<u>161.5507</u>) (<u>0.01905</u>) -7090 (<u>1.488</u>)(1.0502) <u>3600</u>

and Reynolds number (maximum, R-11) - 70900 Similarly, for Reynolds number (minimum, R-113)- 6198 and Reynolds number (maximum, R-113) - 61980 Using Blasius correlation for turbulent flow, in smooth tubes and for Reynolds number \leq 100000,

v²

Darcy's friction factor = $0.316 - f - (\Delta P/L) 2gD$

Re^{0.25} ...f(minimumflow,R-11)=0.034437a**g**, for maximum flow, = 0.019365 and f (minimum flow, R-113) = 0.03561 and, for maximum flow = 0.020027 \therefore ($\Delta P/L$)_{maximum} for R-11 = 0.06178 m/m

and $(\Delta P/L)_{\text{maximum}}$ for R-113 = 0.064167 m/m ... $(\Delta P)_{\text{maximum}}$ = 1.2437 m of R-11 and, is = 1.2918 m of R-113.

F.1.3 Pressure Drop In The Flow Meter

From manufacturer's catalog,

 $(\Delta P)_{flowmeter}$, maximum - 0.3302 m of water column. $(\Delta P)_{flowmeter}$, maximum- 0.223 m of R-11 and $(\Delta P)_{flowmeter}$ - 0.219 m of R-113 F.1.4 Pressure Drop In The Test Annulus

Cross sectional area of the test annulus -

$$\frac{\Pi[(0.0254)^2 - (0.022225)^2]}{4} = 0.000118775 \text{ m}^2.$$

Hydraulic diameter - 0.003175 m.

For R-11, G(minimum)-388 and G(maximum)- 3880.

and for R-113, G(minimum)- 395 and G(maximum)-3950.

For R-11, Reynolds number (minimum)- 2836 and

Reynolds number (maximum) -28361

Similarly, for R-113, Reynolds number (minimum)-2479 and

Reynolds number (maximum) - 24794.

For R-11, Darcy's friction factor (minimum) = 0.0433 and

Darcy's friction factor (maximum) - 0.02435.

For R-113, Darcy's friction factor (minimum)-0.04478 and

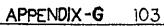
Darcy's friction factor (maximum)= 0.02518.

the $(\Delta P)_{\text{maximum}}$ for R-11 in the test section=1.2437 m. and $(\Delta P)_{\text{maximum}}$ for R-113 in the test section = 1.2918 m. \therefore , the maximum $(\Delta P)_{\text{loop}}$ for R-11 = 2.7 m of R-11 and the maximum $(\Delta P)_{\text{loop}}$ for R-113 = 2.8 m of R-113.

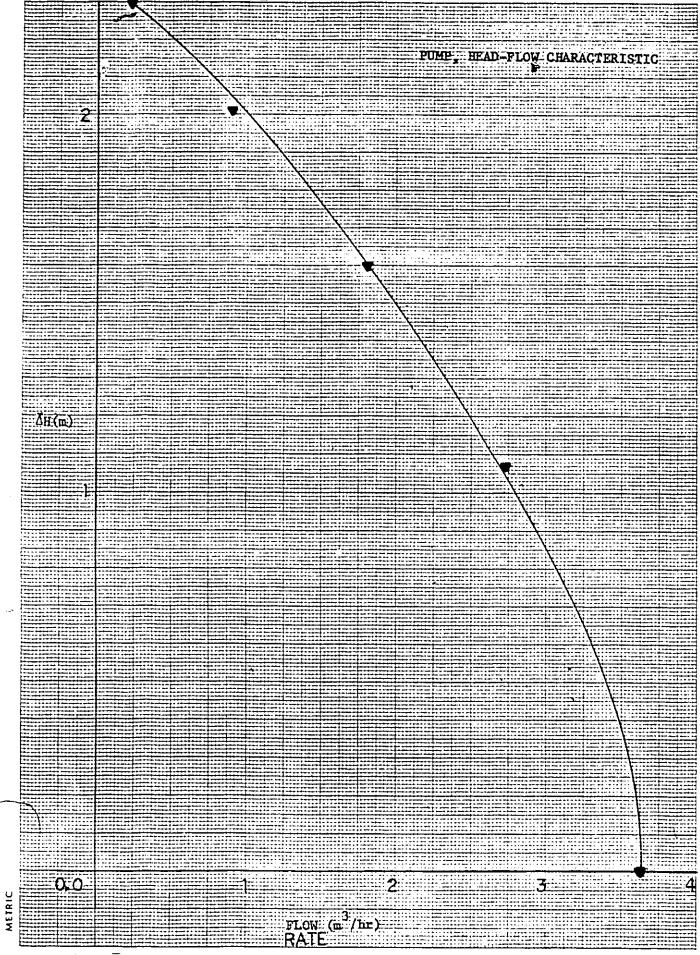
APPENDIX - G

۰.

Pump Model # J-7004-54, Head-Flow Characteristic Curve







APPENDIX - H

"BOIL7" Data Acquisition Program

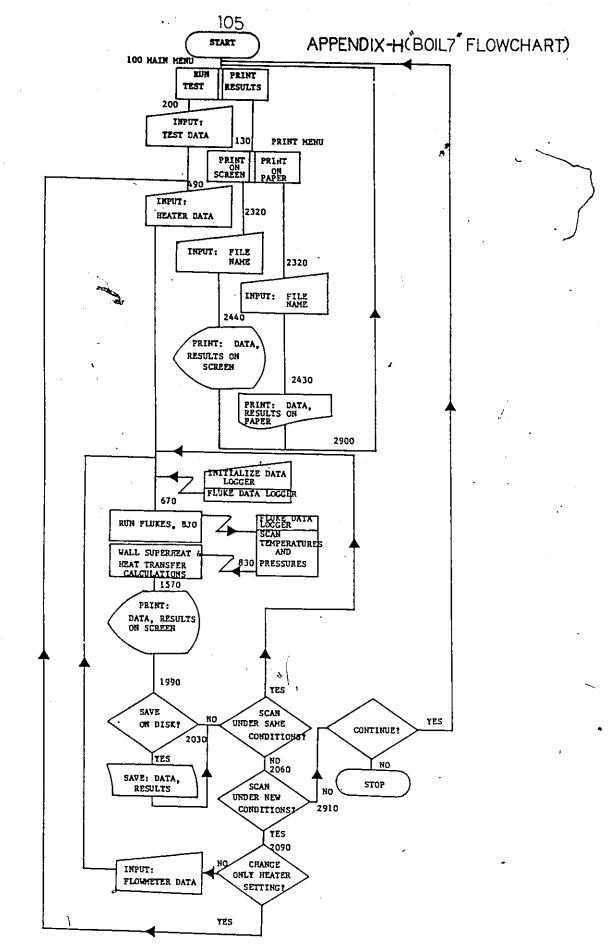
H.1 "BOIL7" Flowchart

H.2 "BOIL7" Variables Nomenclature

H.3 "BOIL7" Program Listing

H.4 "BOIL7" Sample Output





106 APPENDIX-H.2

COMPUTER PROGRAM "BOIL7" VARIABLES NOMENCLATURE

A) NUMERIC VARIABLES

>

Note: In the nomenclature below, the bottommost thermocouple is number one and the top most is number four.

VARIABLE DESCRIPTION

1) AP Atmospheric pressure (cm of mercury).

2) B1, B2, B3, B4 Boiling heat transfer coefficient at the

first, second, third, fourth thermocouple.

3) B5, B6, B7, B8 Convective heat transfer coefficient at first, second, third, fourth thermocouple(W/m2 C)

4) BM Bench mark (-0, if it is the first sequence in the run, else -1).

5) BP Two phase pressure drop in the test section (Pa).

6) BU Two phase pressure drop per unit length (Pa/ cm).

7) C1, C2 Intermediate variables for calculating RC.

8) CF Correction factor for flow rate.

9) CM Heater bottom location with respect to inlet of the glass section (cm).

10) D1, D2 Intermediate variables for calculating fluid density.

11) DD Date of experiment.

12) DE Fluid density at room temperature (kg/m3).

13) DS FluDd density at flow meter inlet (kg/m3).

14) DV Differential pressure transducer (V).

15) FL Loop flow meter reading (%).

16) FR Volumetric flow rate (m3/s).

107 17) HV Heater power (W). 18) LA Latent heat of vaporization (kJ/kg). 19) LK Liquid thermal conductivity (W/m C). 20) LX Heat flux at the test surface (W/m2). 21) M& Month during which the test is being run. 22) MF Mass flow rate (kg/s). 23) MR Maximum radius of cavity in the test section(m). 24) MX Mass flux at the test section annulus (kg/s m2) . 25) P1, P2, P3, P4 Pressure at the first, second, third and fourth thermocouples respectively (Pa) 26) P5 Intermediate variable for calculating system pressure 27) PD Total pressure drop in the test section (Pa). 28) PI Pressure at test section inlet (Pa). 29) PU Single phase pressure drop per unit length (Pa/cm). 30) PV Preheater voltage (V). Thermodynamic wall superheat required for bubble 31) RC growth based on Bergles and Rosehnow's equation (C) 32) RE Reynolds number (#). 33) RS Thermodynamic wall superheat required for bubble growth based on Sato and Matsumura's equation (C). 34) S1, S2, S3, S4 Local wall superheat at first, second, third, fourth thermocouple locations (C). 35) SE Test sequence #. 36) SH Single phase pressure drop in the test section (Pa) Surface tension (N/m). 37) ST Wall temperatures at the first, second, 38) T1, T2, T3, T4 third and fourth thermocouple locations (C).

39) T5, T6, T7, T8 Bulk fluid temperature at the first, second, third and fourth thermocouple elevations (C) 40) TA, TB, TC, TD Fluid saturation temperature at the first, second, third and fourth thermocouple elevations (C) 41) TE Fluid temperature at test section exit (C). 42) TF, TR Non dimensional temperatures. Fluid temperature at test section inlet (C). 43) TI 44) TM Room temperature (C). 45) TN% Test #. Saturation temperature at test section inlet (C). 46) TS 47) TT Cooling water bath temperature (C). 48) TU Fluid temperature at cooler outlet (C). 49) VD Specific volume of vapor (m3/Kg). System pressure output transducer (mV). 50) VI Intermediate variable for calculating dynamic viscosity 51) VL Liquid dynamic viscosity (N s/m). 52) VQ

53) WA Heater wall temperature (C)

B) STRING VARIABLES

ŝ,

- 1) B\$ Strings used to store comments about the run.
- 2) BF\$ Filename (Saving file to disk).
- 3) C\$ If "Y", then continue scan under the same experimental conditions.
- 4) D\$ CHR\$(4).
- 5) F\$ If "Y", then print data, results from the disk.
- 6) H\$ If "S", then print on screen and if "P", then print on paper, the data and results from the disk.

109

7) HR\$

HR\$ If "H", then only heater setting is to be changed, and if "F", then the flow rate setting is to be changed.

8) HS\$ Heater setup time (Hours: Minutes).

9) K1\$ If "Y", then the month input data is correct.

10) K2\$ If "Y", then the test # input data is correct.

11) K4\$ If "Y", then the atmospheric pressure, input data is correct.

12) K5\$ If "Y", then the heater bottom location, input data is correct.

13) K8\$ If "Y", then the loop flow meter reading, input data is correct.

14) K9\$ If "Y", then the preheater voltage input data is correct.

15) L1\$ If"Y", then the heater power input data is correct.

16) L2\$ If"Y", the heater set up time input data is correct.

17) N\$ If "Y", then scan under new experimental conditions.

18) R1\$, R2\$, R3\$, R4\$, R5\$ Strings used to name the file (saving data, results to disk).

19) ST\$ If "Y", store data, results on the disk.

20) T\$ If "Y", run test.

21) VV\$ Filename (retrieving file from data).

22) AK\$, CN\$, RC\$, Z\$ Control string variables for continuing further with the program.

APPENDIX-H.3(PROGRAM LISTING)

```
10 HOME
20 DIH CH(15)
30 D$ - CHR$ (4)
40 PRINT CHR$ (12)
50 PRINT TAB( 10)"FORCED CONVECTION HEAT TRANSFER LOOP"
    PRINT TAB( 10)"DATA ACQUISITION PROCRAM"
PRINT TAB( 10)"BY DINKAR SHIVPRASAD"
70
80 PRINT "** TR IT WORKS --- IT IS A FLUKE**"
90 HOHE
100 INPUT "FOR RUNNING TEST, TYPE Y/N"; T$: PRINT
110 IF T$ - "Y" THEN PRINT "IF THIS IS THE FIRST RUN IN THE SEQUENCE, THEN IT SHOULD BE SING
      LE PHASE FLOW ONLY": PRINT : GOTO 230
120 IF T$ < > "N" THEN GOTO 100
130 INPUT "FOR PRINTING DATA, RESULTS, TYPE Y/N"; F$: PRINT
140 IF F$ - "N" THEN GOTO 2910
150 IF F$ < > "Y" AND F$ < > "N" THEN GOTO 130
160 INPUT "FOR PRINTING ON SCREEN TYPE S, ON PRINTER TYPE P";H$: PRINT
170 IF H$ - "S" THEN GOSUB 2320: GOTO 100
180 IF H$ - "P" THEN GOSUB 2320: PR# 0: GOTO 100
190 IF H$ < > "P" AND H$ < > "S" THEN GOTO 160
200 REH INPUT FOR TEST STARTS
210 REH TEST SECTION MAXH. CAVITY RADIUS IS INPUT IN THE NEXT LINE
220 HR - 0.28 / 1000000
230 INPUT "MONTH-"; MI: PRINT
240 PRINT "HONTH IS ";HZ: PRINT
250 INPUT "MONTH CORRECT? , TYPE Y/N" ;K1$
260 IF K1$ < > "Y" THEN GOTO 230
270 INPUT "TEST #";TNI: PRINT
280 PRINT "TEST # IS"; TNZ: PRINT
290 INPUT "TEST + CORRECT7, TYPE Y/N";K2$
300 IF K2$ = "Y" THEN SE = TN7.: GOTO 320
310 IF K2$ < > "Y" THEN GOTO 270
320 INPUT "ATHOSPHERIC PRESSURE(CH OF HG)"; AP: PRINT
330 PRINT "ATH. PRESSURE(CH OF HG)-"; AP: PRINT
     INPUT "ATH. PRESSURE CORRECT?, TYPE Y/N";K4$
340
350 IF K4$ < > "Y" THEN GOTO 320
360 GOTO 370
370 INPUT "HEATER BOTTON LOCATION WRT INLET TO TEST SECTION(CH)"; CH: PRINT
380 PRINT "HEATER BOTTON LOCATION WRT INLET TO TEST SECTION(CH)=";CH: PRINT
390 INPUT "HEATER LOCATION CORRECT7, TYPE Y/N";K5$
400 IF K5$ < > "Y" THEN GOTU 370
410 INPUT "LOOP FLOW METER READING(7.)";FL: PRINT
420 PRINT "LOOP FLOW HETER READING(7.)=";FL: PRINT
430 INPUT "FLOW HETER READING CORRECT7, TYPE Y/N";K8$
440 IF K8$ < > "Y" THEN GOTO 410
450 INPUT "PREHEATER VOLTAGE(V)"; PV: PRINT
460 PRINT "PREHEATER VOLTAGE(V)-"; PV: PRINT
470 INPUT "PREHEATER VOLTAGE CORRECT?, TYPE Y/N"; K9$
480 IF K9$ < > "Y" THEN GOTO 450
490 INPUT "HEATER POWER(W)";HV: PRINT
500 PRINT "HEATER POWER(W)=";HV: PRINT
510 TNPUT "HEATER POWER CORRECT?, TYPE Y/N";L1$
520 IF L1$ < > "Y" THEN COTU 490
530 INPUT "HEATER SETUP TIME(HH MM)";HS$: PRINT
540 INPUT "REATER SETUP TIME CORRECT?, TYPE Y/N"; L2$
550 IF L2$ < > "Y" THEN GOTO 530
560 HONE
570 D$ = CHR$ (4)
580 REN FLUKE DATA ACQUISITION AND APPLE COMPUTER INTERFACE PROGRAM
590 PRINT "SET FLUKE TO SCAN CHANNELS U TU 11,AT 20 SECOND INTERVALS"
600 PRINT : PRINT
610 PRINT "SET EXTERNAL ENABLE ON ALL DATA": PRINT
620 PRINT : PRINT "TURN OFF ALL SCAN CONTROL BUTTONS"
630 PRINT : INPUT "PRESS RETURN TO CONTINUE";Z$
640 PRINT : PRINT "PRESS INTERVAL ON SCAN CONTROL TO START"
50 PRINT : PRINT : PRINT : PRINT "INITIALIZING DATA LOGGER"
660 PRINT : PRINT "PLEASE WAIT"
670 HOME
68C PRINT D$;"BLOAD FLUKES.BJO,D1"
690 PRINT D$;"IN#2": INPUT " ";A$: PRINT D$;"IN#0"
700 C$ - "012345678901234567890": POKE 254, PEEK (131): POKE 255, PEEK (132):KT - PEEK (255)
      * 256 + PEEK (254) + 1:K17 = K7 + 1
710 CALL 768
720 KK = 32768
730 A - PEEK (KK): 1P A - 65 THEN /10
740 IF A < > 89 THEN KK - KK + 1: GOTU 730
```

```
750 KHZ = KK / 2561 POKE K12, KHZ: POKE K2, KK - KHZ * 256:DD - VAL ( HID$ (C$,2,3))1HH = VAL
       ( HID$ (C$,6,2)):HH = VAL ( HID$ (C$,9,2)):SS = VAL ( HID$ (C$,12,2))
FRINT DD;"";HH;" ";HH;" ";SS;"
  760
  770 KK = KK + 22
  780 KK = KK + 1: IF PEEK (KK) < > 65 GOTO 780
  790 KHX = KK / 256: POKE KIZ, KHZ: POKE KZ, KK - KHZ * 256:CNZ = VAL ( HID$ (C$,2,3)):CH(CNZ) €
        VAL ( HID$ (C$,6,7)):KK = KK + 18: IF PEEK (KK) = 65 GOTO 790
  800 IF PEEK (KK) < > 20 THEN PRINT "ERROR UNPACKING, WILL SCAN AGAIN"; GOTO 710
  810 PRINT : PRINT "COMPLETED SCAN SUCCESSFULLY!"
  820 FOR I - 1 TO 10: CALL - 198: NEXT I
  830 REH DATA TRANSFER BEGINS
  840 \text{ DV} = \text{CH}(0)
  850 VI = CH(1)
  860 \text{ TU} = CH(2)
  870 TE = CH(3)
  880 TI = CH(4)
  890 T1 = CH(5)
  900 \text{ T2} = CH(6)
 910 T3 - CH(7)
 920 \text{ T4} = CH(8)
 930 WA = CH(9)
                                                                                                ١
 940 TT = CH(10)
 950 TH = CH(11)
 960 IF WA > - 120 THEN PRINT "HEATER TEMPERATURE GREATER THAN OR EQUAL TO 120 DEGREES C **
       * WARNING***
 970 REM CALCULATION BEGINS
 980 P5 = (VI * 100 * 6896.5517) / 111-3 + 1315.7895 * AP
 990 TR = (198 - TH) / 471.15
 1000 U1 = 4.031191 + 6.721152 * (TR A 0.3333) + 5.08793 * (TR A 0.6667) - 4.993635 * TR + 4.2
 80343 * (TR > 1.3333)
1010 DE = 137.38 * D1
 1020 PI = P5 + (DE * 9.81 * 9.5 * .0254)
 1030 1F BN - 0 THEN SH = ((6.285 + DV) * 5 * 1000 * 6896.5517) / 143.9 + DE * 18 * .0254 * 9
       .81:BP = 0:PU = SH / (18 * 2.54)
 1040 LF BH = 1 THEN PD = ((6.285 + DV) * 5 * 1000 * 6896.5517) / 143.9 + DE * 18 * .0254 * 9
       .81:BP = PD = PU * (CH + .635)
 1050 BU = BP / (18 * 2.54 - (CH + 0.635))
 1060 P1 = PI - (PU * (CH + 0.635) + BU * 1.2217)
1070 P2 * PI - (PU * (CH + 0.635) + BU * 2.4917)
 1080 P3 = PI - (PU * (CH + 0.635) + BU * 3.7617)
1090 P4 = PI - (PU * (CH + 0.635) + BU * 5.0317)
 1100 TS = - 2568.333 / ( LOG (P1) - 21.04427681) - 245.92511
 1110 TA = - 2568.333 / ( LOG (P1) - 21.04427681) - 245.92511
1120 TB - 2568.333 / (LOG (P2) - 21.0442/681) - 245.93511
1130 TC - 2568.333 / (LOG (P3) - 21.04427681) - 245.92511
1140 TU = - 2568.333 / ( LOG (P4) - 21.04427681) - 245.92511
1150 LX = (HV # 7 * 100 * 100) / (22 * 2.5 * 2.54 * 0.875 * 2.54)
1160 IF LX < = 0 THEN GOTO 1330
1170 S1 = T1 - ( INT (TA * 10) / 10)
1180 T5 = T1 - (TI + .2 * (TE - TI))
1190 B1 = INT (LX / S1)
1200 B5 = INT (LX / T5)
1210 SZ = T2 - ( INT (TB \pm 10) / 10)
                                                                                                . 0
1220 T6 = T2 - (T1 + .4 * (TE - TI))
1230 B2 = INT (LX / S2)
1240 B6 = INT (LX / T6)
1250 S3 = T3 - ( INT (TC * 10) / 10)
1260 T7 = T3 - (T1 + .6 * (TE - TI))
1270 B3 = INT (LX / S3)
1280 B7 - INT (LX / T7)
1290 S4 - T4 - ( INT (TD * 10) / 10)
1300 T8 = T4 - (T1 + .8 * (TE - TI))
1310 B4 = INT (LX / S4)
1320 B8 - INT (LX / T8)
1330 TB = ( INT (TS * 10) / 10) - TI
1340 TF = (198 - TU) / 471.5
1350 D2 = 4.031191 + 6.721152 * (TF A U.3333) + 5.08793 * (TF A U.6667) - 4.993635 * TF + 4.2
      80343 * (TF ^ 1.3333)
1360 US = 137.38 * U2
1370 CF = SQR ((7.238 * US) / (8238 - US))
1380 FR = (6.28 * 3.785 * FL) / (60 * Cr * 1000 * 100)
1390 MF = US * FR
1400 HX - MF * 10000 / 1.187823278
1410 HX = INT (HX * 10) / 10
1420 MF = INT (MF * 1000) / 1000
1430 VL = - 3.9026924 + (1640.191052323 / (TI = 1.8 + 32 + 460))
1440 vQ = EXP (VL) * 0.000672 * 5357
1450 RE = (HX * 3600 * 0.125 * 2.54) / (VQ * 100)
1460 RE = INT (RE)
```

```
1470 LX = INT (LX + 10) / 10
   1480 P1 = INT (P1)
   1490 TA - INT (TA + 10) / 10
   1500 PI = INT (PI)
   1510 VD = .01742 * P1 / (TA + 273.2)
   1520 LK = .08702 - .000278 * (TA - 27)
  1530 ST = (.3873 - .000729 * TA) ~ 4
1540 LA = 173.19 - .4154 * (TA - 45)
  1550 RS = (8 * ST * (TA + 273.16) * LX * 0.001 / (LA * VD * LK)) A .5
  1555 C1 = LX * HR / LK
  1556 C2 = (2 * ST * (TA + 273.16) * 1000000) / (LA * VD * .28 * 1000)
  1560 \text{ RC} = \text{C1} + \text{C2}
   1570 HOHE
   1580 PRINT TAB( U5)"RESULTS OF SCAN": PRINT : PRINT
          VTAB 3: PRINT TAB( 05)"SYSTEM PRESSURE(PA)=";PI: PRINT
  1590
  1600 PRINT TAB( 05)"BULK SUBCOOLING AT INLET TO TEST SEC(C)-"; TB: PRINT
  1610 PRINT TAB( 05)"TEST SECTION TI(C)=";TI;" AND TE (C)=";TE: PRINT
1620 PRINT TAB( 05)"HASS FLUX (KG/H2.S)=";HX: PRINT
  1630 PRINT
                  TAB( 05)"HASS FLOW RATE(KG/S)=";HF: PRINT
                  TAB( U5)"VOL.FLOW RATE(H3/S)=";FR: PRINT
  1640 PRINT
                  TAB( 05)"REYNOLD'S # AT TEST SECTION=";RE: PRINT
TAB( 05)"PRESSURE AT FIRST THERMOCOUPLE LOCATION(PA)=";P1: PRINT
  165U
         PRINT
  1660
         PRINT
         INPUT "PRESS RETURN FOR FURTHER DISPLAY"; AK$ I HOME
  1670

      1870
      INPUT "PRESS RELURM FOR FURTHER DISPLAY"; AK$1 HOME

      1680
      PRINT TAB(03); "THERHOCOUPLE TEMP(C)"; TAB(24); "WALL S'HEAT(C)": PRINT : PRINT

      1690
      PRINT TAB(07); "T1=";T1; TAB(28); "S1=";S1: PRINT

      1700
      PRINT TAB(07); "T2=";T2; TAB(28); "S2=";S2: PRINT

      1710
      PRINT TAB(07); "T3=";T3; TAB(28); "S3=";S3: PRINT

      1720
      PRINT TAB(07); "T4=";T4; TAB(28); "S4=";S4: PRINT : PRINT

      1720
      PRINT TAB(04); "U411 TEMP DIFF (C)"; DUINT : DEINT

  1730 PRINT TAB( 08); "WALL TEMP. DIFF.(C)"; PRINT : PRINT
1740 PRINT TAB( 07); "DT1="; T3; TAB( 28); "RS1(C)= "; RS
  1750 PRINT TAB( 20);"DT2="; TAB( 28);T6: PRINT
  1760 PRINT TAB( 20);"DTJ="; TAB( 28);T7; PRINT
1770 PRINT TAB( 20);"DT4="; TAB( 28);T8; PRINT
        INPUT "PRESS RETURN FOR FURTHER DISPLAY"; AKS: HOME
  1780
                  TAB( 05)"HEAT FLUX (W/H2)=";LX: PRINT
  1790 PRINT
        FRINT TAB( 04);"BOILING HT.TR COEF"; TAB( 25);"CONV HT.TR COEF": PRINT : PRINT
  1800
        PRINT TAB( 08); "AT TC#1(W/H2.C)=";B1; TAB( 32); B5; PRINT
PRINT TAB( 08);"AT TC#1(W/H2.C)=";B1; TAB( 32); B5; PRINT
PRINT TAB( 08);"AT TC#2(W/M2.C)=";B3; TAB( 32); B6; PRINT
PRINT TAB( 08);"AT TC#3(W/H2.C)=";B3; TAB( 32); B7; PRINT
  1810
  1820 PRINT
  1830
 1840 PRINT
                  TAB( U8); "AT TC#4(W/M2.C)=";84; TAB( 32);88; PRINT
        INPUT "PRESS RETURN FOR FURTHER DISPLAY"; AK$: HOME
 1830
 1860
         PRINT
                  TAB( U5)"COOLER OUTLET TEMP(C)=":TU: PRINT
        PRINT
                  TAB( 05)"CW BATH TEMP(C)-";TT: PRINT
 1870
                                                                                           ĝ,
 1880
        PRINT TAB( U5)"HEATER TEMP(C)=";WAI PRINT
 1890 PRINT TAB( 05)"ROON TEMP(C)-";TH: PRINT
 1900 RS - INT (RS - 10) / 10
 1910 RC = INT (RC * 10) / 10
 1920 PRINT TAB( ) "SUPHT REQD & TC1(C)-";"TD";RS;" ";"CAV";RC: PRINT
 1930 PU = INT (PU * 100) / 100
 1940 PRINT TAB( ))"SINGLE PHASE UP/DZ (Pa/H) = ";PU = 100: PRINT
 1950 BU - INT (BU * 100) / 100
 1960 PRINT TAB( 5)"TWO PHASE DP/DZ (PA/H) = ";BU * 100; PRINT
1960 PRINT "VD= "; INT (VD * 100) / 100;" ST= "; INT (ST * 10000) / 10000;" DE= "; INT (DE);
"PRESS_DROP="; INT (PD);" "; INT (SH)
 1980 INPUT "PRESS RETURN TO CONTINUE";RC$
 1990 HOME
 2000 INPUT "TYPE Y/N FOR STORING DATA, RESULTS ON DISK"; ST$: PRINT
 2010 IF ST$ - "Y" THEN INPUT "COMMENTS ABOUT THE RUN?"; B$: GOSUB 2140: GOTO 2030
 2020 IF ST$ < > "Y" AND ST$ < > "N" THEN GOTO 2000
 2030 HOME : INPUT "TYPE Y/N FOR CONTINUING SCAN UNDER SAME EXPT CONDITIONS";CS$: PRINT
 2040 IF CS$ = "Y" THEN SE = SE + 0.01:BM = 1:PU = PU: GOTO 650
 2050 IF CS$ < > "Y" AND CS$ < > "N" THEN GOTO 2030
 2060 INPUT "TYPE I/N FOR SCAN UNDER NEW EXPT. CONDITIONS";NS$: PRINT
 2070 IF NS3 = "N" THEN COTO 2910
 2080 IF NS$ < > "Y" AND NS$ < > "N" THEN GOTO 2060
 2090 INPUT "TO CHANGE ONLY THE HEATER POWER TYPE H. THE FLOW RATE TYPE F ";HR$
 2100 IF HR$ - "H" THEN TNZ = TNZ + 1:SE = TNZ: HOME : GOTO 490
 2110 77 HR3 = "F" THEN TNL = TNL + 1:SE = TNL: HOME : PRINT "THE FIRST RUN MUST BE SINGLE PH
       ASE FLOW": BM = O: PRINT : INPUT "FLOW HETER Z= ";FL: PRINT : INPUT "RESET TIME = ";HS$: GOTO
 2120 TNL = TNL + 1:SE = TNL: HOME : PRINT "IF THIS IS THE FIRST RUN IN THIS SEQUENCE, THEN IT
       SHOULD BE SINGLE PHASE FLOW": BM - U: GOTO J60
 2130 IF HR$ < > "Y" AND HR$ < > "N" THEN GOTO 2090
 2140 REM SUBROUTINE FOR STORING DATA, RESULTS
 2150 D$ = CHR$ (4)
 2160 PRINT D$;"CATALUG, D2"
 2170 PRINT "PILENAME IS B.";DD;".";SE
 2180 R13 - "B"
2190 R2$ = "."
```

```
B: PRINT MX: PRINT RE: PRINT LX: PRINT B1: FRINT B2: PRINT B3: PRINT B4
    2270 PRINT T1: PRINT T2: PRINT T3: PRINT T4: PRINT T5: PRINT T6: PRINT T7: PRINT T8: PRINT B
         5: PRINT B6: PRINT B7: PRINT B8: PRINT RS: PRINT PU * 100: PRINT BU * 100
    2280 FRINT RC
    2290 PRINT D$;"CLOSE"
    2300 KETURN
   2310 REM SUBROUTINE FOR PRINTING FILE
   2320 D$ = 'CHR$ (4)
   2330 FRINT D$;"CATALOG, D2"
   2340 PRINT : INPUT "FILENAME:";VV>
   2350
         HOME
   2360 PRINT D$;"OPEN";VV$
   2370 PRINT D$;"READ";VV3
        INPUT MA: INPUT DD: INPUT HH: INPUT HH: INPUT B$: INPUT AP: INPUT TH: INPUT PV: INPUT H
V: INPUT CH: INPUT FL: INPUT TA: INPUT TI: INPUT TE: INPUT TU: INPUT TT: INPUT HS$
   2380
   2390 INPUT PI: INPUT P1: INPUT FR: INPUT MF: INPUT S1: INPUT S2: INPUT S3: INPUT S4: INPUT T
        B: INPUT MX: INPUT RE: INPUT LX: INPUT B1: INPUT B2: INPUT B3: INPUT B4
   2400 INPUT T1: INPUT T2: INPUT T3: INPUT T4: INPUT T5: INPUT T6: INPUT T7: INPUT T8: INPUT B
        5: INPUT B6: INPUT B7: INPUT B8: INPUT RS: INPUT PU: INPUT BU
   2410 INPUT RC
  2420 PRINT DAS"CLOSE"
2430 IF H$ = "P" THEN PRINT "POSITION PAPER IN PRINTER": INPUT "PRESS RETURN TO CONTINUE";C
  2440 PRINT "###FILENAME IS= ";VV$
2450 PRINT "SCAN HONTH= ";M7;" ";
  2460 FRINT "SCAN DATE=";DD;"
                                   SCAN TIME=";HH;":";HH
  2470 PRINT "COMMENTS? ";B$
  2480 PRINT "ATH.PRESSURE(CH OF HG)=";AP;" ";
        PRINT "ROOM TEMP(C)=";TH
  2500 IF H$ = "S" THEN INPUT "PRESS RETURN FOR FURTHER DISPLAY";AK$: HOME
  2510 PRINT "SYSTEM PRESSURE(Pa)=";PI;"
2520 PRINT "INLET SUBCOOLING(C)=";TB
                                             ";
  2530 PRINT "FLUID TEMP AT TEST SEC INLET(C)-";TI;" ";
        PRINT "AND AT OUTLET(C)=";TE
       PRINT "HASS FLUX IN TEST SEC(KG/H2.5)=";HX;" ";
  255u
  2560 PRINT "REYNOLD'S # AT TEST SEC=";RE
      PRINT "MASS FLOW RATE(KG/S)=";HF;"
  2570
 2580 PRINT "VOL.FLOW RATE(M3/S)=";FR
      PBINT "PREHEATER VOLTAGE(V)=";PV;" ";
PRINT "HEATER POWER(W)=";HV;" SET TIME=
 2590
 2600
                                                   ":HS$
       PRINT "HEATER BOTTOM LOCATION WRT TEST SEC INLET(CH)=";CH
 261U
       PRINT "PRESSURE AT FIRST THERHOCOUPLE ELEVATION(Pa)=";P1
 2620
       PRINT "SATN. TEMP AT FIRST THERMOCOUPLE ELEVATION(C)-";TA
 2000
       IF H$ - "S" THEN INPUT "PRESS RETURN FOR FURTHER DISPLAY"; AK$: HOME
 2640
       PRINT "TC#1 TEMP(C)=";T1;" ";
 265u
       PRINT "WALLI SUPHT TEMP(C)=";S1
 2660
       PRINT "REQU SUPHT(C)=";"THERHUDYNAHIC ";KS;"CAVITY RAD ";RC
 2670
       PRINT "TEMP DIFF (C) = "To
 2680
 2690
       PRINT "TC#2 TEMP(C)=";T2;"
       PRINT "WALL2 SUPHT TEMP(C)=";S2
 2700
 271u
       PRINT "TEMP DIFF#2 = ";T6
       PRINT "TCJ3 TEMP(C)=";T3;"
 2720
       PRINT "WALLS SUPHT TEMP(C)=";S3
 273u
      PRINT "TEMP DIFF#3 - ";T7
 2740
2750
       PRINT "TC#4 TEMP(C)=";T4;"
     PRINT "WALL4 SUPHT TEMP(C)=";54
2760
2770
      PRINT "TEMP DIFF#4 = ";T8
      LF H$ - "S" THEN INPUT "PRESS RETURN FOR FURTHER DISPLAY"; AK$: HOME
2780
      PRINT "HEAT FLUX (W/HZ)= ";LX;" (DP/DZ)1P = ";PU;" (DP/DZ)2P = ";BU
2790
      PRINT "BOILING HEAT TRANSFER COEFF AT TC#1 LUC. (W/M2.C)-"; B1
2800
      PRINT "CONV. HEAT TRANSFER CUEFF AT TC+1 LOC. (W/HZ.C)-";BD
2810
      PRINT "BUILING HEAT TRANSFER COEFF AT TC#2 LOC. (W/H2.C)=";82
2820
2830 PRINT "CONV.HEAT TRANSFER COEFF AT TC#2 LOC. (W/HZ.C)=";86
      PRINT "BOILING HEAT TRANSFER COEFF AT TU#3 LOC. (W/M2.C)=";83
      PRINT "CONV.HEAT TRANSFER CUEFF AT TC#3 LOC. (W/H2.C)=";B7
2850
      PRINT "BUILING HEAT TRANSFER COLFY AT TC#4 LUC. (W/M2.C)="; 84
2860
      PRINT "CONV.HEAT TRANSFER CUEFF AT TC+4 LOC. (W/HZ.C)-";B8
2870
      PRINT "PLUID TEMP AT COULER OUTLET(C)-";TU;"
2880
      PRINT "CW BATH TEMP(C)=";TT: PRINT
289u
2900
      RETURN
```

V: PRINT CM: PRINT FL: PRINT TA: PRINT TI: PRINT TE: PRINT TU: PRINT TT: PRINT HS\$ 2260 PRINT PI: PRINT P1: PRINT FR: PRINT MY: PRINT S1: PRINT S2: PRINT S3: PRINT S4: PRINT T

2250 PRINT MZ: PRINT DD: PRINT HH: PRINT HM: PRINT B\$: PRINT AP: PRINT TH: PRINT PV: PRINT H

2240 PRINT D\$;"WRITE";BF\$

2220 BF\$ = R1\$ + R2\$ + R4\$ + R2\$ + R5\$ 2230 PRINT D\$;"OPEN"; BF3

2210 R5\$ - STR\$ (SE)

2200 R4\$ - STR\$ (UD)

2910 INPOT "TYPE I/N TO CONTINUE";CN\$ 2920 IF CN\$ = "Y" THEN GOTO 100 2930 IF CN\$ < > "Y" AND CN\$ < > "N" THEN GOTO 2910 2940 END

..

~

ð

.

1

ģ

C-1-

115

APPENDIX- H.4 (SAMPLE OUTPUT)

IRRONANPILENAME IS- 8.9.35.01 SCAN MONTH= 1 SCAN DATE=y SCAN TIME+0:26 COMMENTS? SITES JUST QUENCHED. ATH.PRESSURE(CH OF HG)=75 ROOH TEHP(C)=25.8 SYSTEM PRESSURE(Pa)=306234 INLET SUBCOULING(C)=22.4 YLUID TEHP AT TEST SEC INLET(C)=36.9 AND AT OUTLET(C)=38 MASS FLUX IN TEST SEC(KG/H2.S)=388.6 REYNOLD'S # AT TEST SEC=3240 MASS FLOW RATE(KG/S)=.046 VUL.FLOW RATE(H3/S)=3.18970317E-05 PREHEATER VOLTAGE(V)=0 HEATER FOWER(W)=70 SET TIME= 00 23 HEATER BOTTOH LOCATION WRT TEST SEC INLET(UN)=29 PRESSURE AT FIRST THERMOCOUPLE ELEVATION (FA)= 300587 SATN. TEMP AT FIRST THERMOCOUPLE ELEVATION(C)=58.7 TC#1 TEMP(C)=66.5 WALL1 SUPHT TEMP(C)=7.80000001 REQD SUPHT(C)-THERMODYNAMIC 1.6CAVITY RAD 44.2 TEMP DIFr#1(C) = 29.38 TC#2 TEMP(C)=67.5 WALL2 SUPHT TEMP(C)=8.90000001 TEHP DIFF#2 = 30.16 TC#3 TEMP(C)=06 WALL3 SUPHT TEMP(C)=/.4000001 TEMP DIFF#3 = 28.44 TC#4 TEMP(C)=65.8 WALL4 SUPHT TEMP(C)=7.20000002 TEMP D1FF#4 = 28.02 HEAT FLUX (W/HZ)= 15781.8 (DP/UZ)1P = 18125 (UP/DZ)2P = 22611 BOILING HEAT TRANSFER COEFF AT TC#1 LOC. (W/H2.C)=2023 CONV.HEAT TRANSFER COEFF AT TC#1 LOC. (W/H2.C)=53/ BOILING HEAT TRANSFER COEFF AT TC#2 LUC. (W/H2.C)=17/3 CONV.HEAT TRANSFER CUEFF AT TC#2 LOC. (W/H2.C)=523 BOILING HEAT TRANSFER CUEFF AT TC#3 LOG.(W/H2.C)=2132 CUNV.HEAT TRANSFER COEFF AT TO#3 LUC. (W/H2.C)=554 BUILING HEAT TRANSFER COEFF AT TC#4 LUC.(W/H2.C)=2191 CONV.HEAT TRANSFER COEFF AT TC#4 LOC. (V/M2.C)=563 > FLUID TEMP AT COOLER OUTLET(C)=36.5 CW BATH TEMP(C)=34.1 ***FILENAME IS= B.8.26.04 SCAN MONTH= 1 SCAN DATE=8 SCAN TIME=22:54 COMMENTS? ALL SITES QUENCHED. ATH.PRESSURE(CH OF HG)=/6 ROOM TEMP(C)=25.9 SYSTEM PRESSURE(Pa)=368073 INLET SUBCUOLING(C)=28.5 PLUID TEMP AT TEST SEC INLET(C)=37.7 AND AT OUTLET(C)=39.1 HASS FLUX IN TEST SEC(KG/HZ.S)=388.1 REYNOLD'S # AT TEST SEC=3260 MASS FLOW RATE(KG/S)=.046 VOL.FLOW RATE(H3/S)=3.19530821E-05 PREHEATER VOLTAGE(V)-U HEATER POWER(W)-93 SET TIME- 22 39 HEATER BUTTOM LUCATION WRT TEST SEC INLET(CH)=29.9 PRESSURE AT FIRST THERMOCOUPLE ELEVATION(Pa)=350970 SATN. TEMP AT FIRST THERMUCUUPLE ELEVATION(C)-65.4 TC#1 TEMP(C)=/4.8 WALLI SUPHT TEMP(C)=9.40000002 REQU SUPHT(C)-THERMODYNAMIC 1.7CAVITY RAD 36.8 TEMP DIFF#1(C) = 36.82 TUP2 TEMP(C)=74.3 WALL2 SUPHT TEMP(C)=8.90000002 TEMP DIFF#2 = 36.04 TC#3 TEHP(C)=75.8 WALL3 SUPHT TEHP(C)=10.4 TEMP DIFF#3 - 31.26 TC#4 TEHP(C)=70.8 WALL4 SUPRT TEHP(C)=5.40000002 TEMP DIFF#4 - 31.98 HEAT FLUX (W/H2)= 2096/.3 (UP/DZ)1P = 22855 (DP/UZ)2P = 10202 BUILING HEAT TRANSFER COEFF AT TU#1 LUC. (W/H2.C)=2230 CONV.HEAT TRANSFER CUEFF AT TC#1 LOC. (W/HZ.C)=569 BOILING HEAT TRANSFER CUEFF AT TC#2 LOC. (W/H2.C)=2355 CUNV.HEAT TRANSFER COEFF AT TU#2 LUC. (W/H2.C)=381 BUILING HEAT TRANSFER COEFF AT TC#3 LUC. (#/H2.C)=2016 CONV.HEAT TRANSFER CUEFF AT TC#3 LOC. (W/M2.C)=562 BOILING HEAT THANSFER CUEFF AT TC#4 LOC.(W/HZ.C)=3882 CONV.HEAT TRANSFER COEFF AT TC#4 LUC. (W/H2.C)=650 FLUID TEMP AT COOLER OUTLET(C)=38.5 CW BATH TEMP(C)=28

-

~~~

# APPENDIX - I

# List Of Equipment and Instrumentation

,

ł

#### APPENDIX-I

#### LIST OF EQUIPMENT AND INSTRUMENTATION

1.<u>Cartridge Heater</u>, Model # H1-3, Fast heat, "Hi-Temp", 7.874 mm diameter, 63.5 mm heated length, 76.2 mm sheath length, 141.05 KW/m2 heat flux, 225 W, at 120 V. Acrolab Instruments, Windsor, Ontario.

2.<u>Computer</u>, APPLE II Plus with RS 232 interface card, Program language APPLE BASIC, Apple Computer, Inc., 10260 Bandley Drive, Cupertino, California.

3.<u>Constant Current Supply</u>, Model # PS-KIT-1, input 12V, output 1.5 mA, Omega Engineering Company, Stamford, Connecticut.

4.<u>Constant Temperature Bath</u>, Model # K-40, 115 V, 800 W, Messerate-Werk Lauda, W. Germany.

5.<u>Data\_Logger</u>, Fluke Data Logger, Model # 2240 C, John Fluke Manufacturing Co., Everett, Washington.

6.<u>Dial Pressure Gage</u>, Model # R07-200-RNKA, 0-11 bar(gage).

C.A Norgren Co Inc., Littleton, Colarado.

7.<u>Differential Pressure Transducer</u>, Model # PX83-005 DV, 0.345 bars differential, span 143.9 mV at 1.5 mA, Omega Engineering Company, Stamford, Connecticut.

8.<u>Glass Pipe</u>, Borosilicate glass pipe, PS1/ 18, I.D. 25.4 mm, maximum working temperature 300 degrees C, maximum <sup>)</sup>working pressure 7.91 bars, Pegasus Industrial Specialities Ltd, Agincourt, Ontario.

9.<u>Filter Drier</u>, Model # ALCO ASD 45S6-VV, Mueller Brass Co., Port

Huron, Michigan.

10.<u>Flowmeter</u>, Model # FL-1504 A, with flow range 0.628 US gpm-6.28 US gpm for water and with graduations at an increment of 0.1256 gpm. Omega Engineering Company, Stamford, Connecticut. 11.<u>Preheater</u>, Model # 220 1968, 282.6 mm long, oil immersion heater, 300 W, 120 V, Temro Products Inc., Winnipeg, Manitoba. 12. <u>Pump</u>, Model # J-7004-54, maximum flow rate 7.5 US gpm, maximum head 5.18 m of water, Net Positive Suction Head (required) 0.1524 m, Cole Parmer Instrument Company, Chicago, Illinois.

13.<u>Pressure Transducer</u>, Model # PX 82-100 GV, maximum pressure 7.9 bars, 111.3 mV span at 1.5 mA, Omega Engineering Company, Stamford, Connecticut.

14. Printer, Model # 26-1168, TRS-80 Line printer VIII, Tandy Electronics Ltd., Barrie, Ontario.

15.<u>System Pressurizer</u>, Model # ABO1B3T1A1K, 0.000946 m3 size, 206.9 bars, Parker Fluid Power, Des Plaines, Illinois.

16.<u>Thermocouple Plugs</u>, Model # OPNE-14, with 2 self sealing neoprene rings, Omega Engineering Company, Stamford, Connecticut. 17.<u>Vacuum Pump</u>, Model # 1399, The Welch Scientific Company, Skokie, Illinois.

18.<u>Valve</u>, 19mm, Model # 901 A, ball valve, Jenkins Company, USA.
19.<u>Variac</u>, Model # W5MT3, 0-140 V, General Radio Company, Concord, Massachussets.

20.<u>Wattmeter</u>, Model # 880, 0-250 W, Simpson Electric Company, Chicago, Illinois.

#### VITA AUCTORIS

- 1958 Born in Tuticorin, India on November 25. 1975 Completed the Secondary School Certificate from Maharashtra Board, through S.I.W.S High School, Bombay, India. 1977 Completed the Intermediato Science examination from Bombay University, through S.I.E.S College of Arts, Science and Commerce, Bombay, India. 1981 Completed the Bachelor of Engineering from Bombay University, through Victoria Jubilee Technical Institute, Bombay, India. 1981 Joined National Organic Chemical Industries Limited, Bombay, India as Trainee Engineer, and held-positions as Assistant Maintenance Engineer, Project Engineer.
- 1989 Currently a candidate for the degree of Master of Applied Science at University Of Windsor.

たまでゆりる